*Int. J. Multiphase Flow*, Vol. 2, pp. 273–306. Pergamon/Elsevier, 1975. Printed in Great Britain.

# THE INTERRELATION BETWEEN VOID FRACTION FLUCTUATIONS AND FLOW PATTERNS IN TWO-PHASE FLOW

OWEN C. JONES, JR.
Argonne National Laboratory, Argonne, Illinois 60439, U.S.A.

and

NOVAK ZUBER
Nuclear Regulatory Commission, Washington, D.C., U.S.A.

(*Received* 22 *March* 1974)

**Abstract**—A fast response, linearized X-ray void measurement system has been used to obtain statistical measurements in normally fluctuating air–water flow in a rectangular channel. It is demonstrated that the probability density function (PDF) of the fluctuations in void fraction may be used as an objective and quantitative flow pattern discriminator for the three dominant patterns of bubbly, slug, and annular flow. This concept is applied to data over the range of 0.0 to 37 m/sec mixture velocities to show that slug flow is simply a transitional, periodic time combination of bubbly and annular flows. Film thicknesses calculated from the PDF data are similar in magnitude in both slug and annular flows. Calculation of slug length and residence time ratios along with bubble lengths in slug flow are also readily obtainable from the statistical measurements. Spectral density measurements showed bubbly flow to be stochastic while slug and annular flows showed periodicities correlatable in terms of the liquid volume flux.

## INTRODUCTION

In the design and analysis of two phase systems, little attention has been paid to the inherent discreteness of the flow field. Analyses have usually considered only the two extremes of fully mixed, homogeneous flow or fully separated flow. While such analyses are important in defining limiting behavior or in qualitatively predicting system performance, they usually fall short of general design utility. Empirical or semiempirical methods using analyses as guides have thus found wide application in this field. Ishagai, *et al.* (1965) demonstrated that the heterogeneous nature of two-phase flow could be important. They showed that a measurement of the flow rates of individual components through an orifice could be calculated from a measurement of the fluctuating pressure drop. The inherent unsteadiness of these flows has been adequately demonstrated by a number of workers such as Akagawa (1964), Lackme (1964) and Neal & Bankoff (1963), and is readily testified to by an experimenter who has tried to measure differential pressures along a duct carrying two-phase flow.

Delhaye (1969) expressed the field equations in terms of statistical averages, Hewitt *et al.* (1970) and Telles & Dukler (1970) have examined certain statistical characteristics of two-phase flows. The problems of inaccuracies in void fraction measurements caused by fluctuations was recognized by Jones (1970) and by Harms & Forrest (1971). The problems associated with analytically considering the discreteness are formidable as reviewed by Kocamustafaogullari (1971). The major problem lies in the fact that in general, two-phase flow is a macroscopic conglomeration and may not be treated on the whole as a single fluid. Hence, point differentials are not adequate in themselves to completely describe the system behavior because, at one instant one phase exists and one set of relations would hold, whereas, at the next instant the fluid would change and the alternate set of equations would govern. It is improbable that the correct and complete set of field equations has yet been identified, although the area averaging techniques presented by Kocamustafaogullari (1971) appear to be the most complete to date for the one-dimensional case. Considering the large bulk of literature in this field, however, it is surprising that more attention has not been paid to the more fundamental characteristics inherent in this phenomenon.

The purpose of this paper is to emphasize the need for expanded analytical and experimental efforts in this area, and to present experimental data which allow more fundamental information

to be obtained about two-phase flow in general. The results include a simplification of overall flow pattern classification suggested by the statistical data and the development of an objective flow pattern discriminator for the three major classifications; bubbly flow, slug flow and annular flow. The data suggest that in the overall view neglecting the fine structure, slug flow is simply a transitional flow, periodically fluctuating between bubbly flow and annular flow, and thus is simply a recurring time combination of these latter two independent regimes. The simplification thus demonstrated provides insight for an uncluttered synthesis of a multi-dimensional model of two-phase flow which otherwise appears to be a chaotic and confusing situation.

## EXPERIMENTAL EQUIPMENT

A complete description of the experimental setup is given by Jones (1970, 1973). The test section used was fabricated from flat, lucite plates separated by lucite spacers machined to form a rectangular flow passage calibrated to measure $0.498 \times 6.350$ cm. The Plexiglas plates had porous stainless steel plates mounted flush with the inside surface to form thin sections 6.350 cm square through which air or water could be injected. Four of these porous inlet sections were centered on 0.610 m intervals on both flats of the channel beginning at 0.610 m from the exit of the 3.05 m long duct. The entrance and exit consisted of sharp edged expansion and contraction to plenum areas about 5 cm and 12.7 cm in dia., respectively. For the bubbly flow runs, air was injected through the porous plates 1.22 m from the exit with water injected through the inlet plenum. This was required in order to obtain bubble sizes by shear which were smaller than the duct spacing. For the other runs, air was injected into the inlet plenum while water was injected through the porous plates 2.44 m from the exit. X-ray void fraction measurements were taken through a lateral "window" at the duct exit formed by machining a slot 1.27 cm high, and as wide as the channel, but leaving 0.95 cm of Plexiglas left as a pressure barrier to the flow. Air was obtained through a carefully regulated supply with 0.9 $\mu$m filtering. Water was recirculated through air–water separators and pumped through a 30 $\mu$m filter to the test section. Flow rates were measured between the supply and the channel by variable area logarithmic rotameters having accuracies of 0.5 per cent of reading for the water, and 1 per cent of reading for air.

The X-ray system used to measure void fraction was a modified, Phillips Norelco 50 kV, 50 mA diffraction unit. The tube used was a General Electric CA-7 700-W, triple-port tube having a tungsten target. Operating voltages were 35 kV at currents of 20 mA which were found to maximize signal-to-noise ratio and sensitivity. Power was obtained through a 208–240 vac, 60 Hz, regulated supply. The X-ray tube was shielded and provided with two, collimated, horizontal X-ray beams, one used as a reference. The test section beam was narrowly collimated so as to be emergent at $0.25 \times 2.54$ mm. Dispersion increased the size to approximately $1.27 \times 3.8$ mm at the test section. Due to extremely low intensity of this small beam and the need for fast response time, the beam was not recollimated before it entered the photomultiplier tube. The intensity of these beams was measured using Dumont type 6292 photomultipliers fitted with thallium-activated, sodium iodide crystals completely covering the transparent end. The anode current of each tube was amplified through a Philbrick P75AU operational amplifier having water-stabilized, logarithmic diode network feedback to each input. This signal was found to be linear within $\pm 2$ per cent voids and reproducible for steady-state measurements within 1.7 per cent voids for attenuation layers orientated perpendicular to the X-ray beam. This accuracy was only obtained after precautions were taken to reduce the 60 Hz ripple normally encountered in X-ray beam intensities to a negligible amplitude. It was determined that this ripple was due to variations in the thermal emission of electrons from the X-ray tube anode. These variations were caused by ripple on the rectified, high voltage supplied to the tube even though 50 $\mu$f capacitance was placed directly between this high voltage and ground. In a low voltage circuit, this type of problem could be cured by filtering, since the emission current was driven only by a $\sim 10$ V differential. But the difficulty in this case was that this 10 V differential was at a potential up to 35 kV with respect to ground. Filtering was accomplished by direct insertion of a 25 V, solid state diode bridge in this

emission circuit, along with 80 k$\mu$f capacitance. These filtering components were simply isolated from ground within the high tension environment of the transformer–rectifier oil bath. The resulting system had 60 Hz ripple less than ~3 per cent voids in amplitude. The response time to a 100 per cent step change in void fraction was found to be less than ~1 msec.

Approximately 60 runs were obtained, each one requiring 8–16 hr to complete all the measurements described by Jones (1973). (These measurements included differential pressures, transverse void profiles, and small dimension profiles of void fraction, liquid volume flux and interface passage frequency.) The characteristics of a particular flow regime are going to be noticed first at the duct centerline. Thus, the disappearance of liquid bridging, when slug flow becomes annular flow, would occur first at the centerline and then spread outward toward the sidewalls. Likewise, in slug flow the predominant frequencies will be identical in most regions of the duct so centerline measurements are representative of the whole channel. In addition, if the bubbles in bubbly flow are uniform in space, the only differences in these statistical measurements due to position changes would be a change in the level of the void fraction and not in the amplitudes of the fluctuations. It thus appeared to be a reasonable compromise between time requirements and the desire for more detailed information to take data only at the channel centerline.

A Hewlett Packard model 5450A Fourier Analyzer was used to obtain the statistical data which were then analyzed further and plotted on a combined PDP-10, CDC-6600, CDC-7600 computer system. The probability distribution function (PDF) and the power spectral densities were obtained by the technique of successive averaging. A void–time record was read by the analyzer, the PDF and PSD of this record were then obtained and added to the previous results and then displayed on an oscilloscope screen. This process was continued until these were found to be stationary at which point proper normalization was completed, and the results punched on paper tape and saved for further analysis. The time averaged centerline void fraction was also measured using a Hewlett–Packard model 2401C integrating digital voltmeter, obtaining between 10 and 30 each of 10-sec integrated values. The adequacy of the method of obtaining the PDF data was checked by comparing the first moment of the PDF with the time-integrated, averaged values of the void fraction. The results are shown in figure 1. The system noise was found to be Gaussian in nature as shown in figure 2, with a standard deviation of 2.2 per cent voids, but slightly variable with void fraction due to the intensity variations of the signal.

## CONCEPTUAL DESCRIPTION

Before discussing the data obtained, it is worthwhile to describe what the PDF yields from a physical standpoint. If the probability that the void fraction $\alpha$ is less than some specific value is given by $P(\alpha)$, then $dP(\alpha)/d\alpha = p(\alpha)$ represents the probability per unit void fraction that the

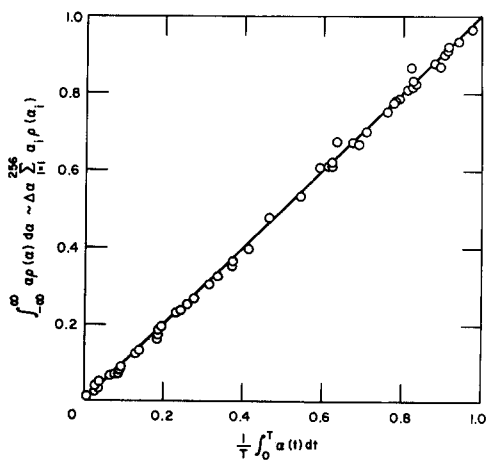


Figure 1. Comparison of time averaged void measurement with first moment of the PDF.

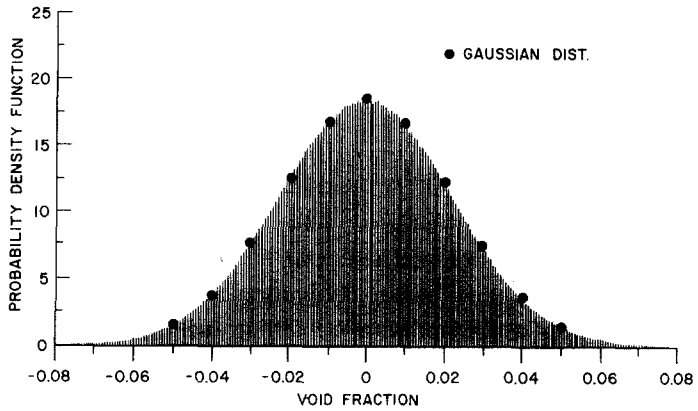


Figure 2. Probability sample of void signal for all water ($\alpha = 0$).

void fraction lies between the values of $\alpha$ and $\alpha + d\alpha$. Consider a void–time trace record where the void scale is broken into equal increments of $\Delta\alpha_i$ and the time scale broken into equal increments of $\Delta t_j$. If during the total time interval $T$ the void fraction is seen to be in $\Delta\alpha_i$ a total of $n_i$ times then

$$\frac{n_i/N}{\Delta\alpha_i} = \frac{1}{\Delta\alpha_i} \sum_{j=1}^{n_i} \frac{\Delta t_j}{T}. \qquad [1]$$

If the flow is bubbly, a large count ratio, $n_i/N$ would occur at low void fraction while small ratios would exist in $\Delta\alpha_i$'s at higher values of $\alpha$. The opposite would happen in annular flow. Since the ratio $\Sigma\, t_i/T$ is the probability that the void fraction lies within the given interval $\Delta\alpha_i$, it is seen that

$$\lim_{\Delta\alpha_i \to 0} \frac{1}{T\Delta\alpha_i} \sum_{j=1}^{n_i} \Delta t_i \to p^1(\alpha) \qquad [2]$$

represents the probability density function of the particular record examined. This has been denoted record number 1 as shown by the superscript in [2]. The PDF has local high values at low mean void fractions in bubbly flow, and at high mean void fractions in annular flow.

The PDF for the particular record given by [2] will have a particular configuration dependent on the nature of the flow passing through the X-ray beam during the sample time. The next time period during which time another record is taken and $p^2(\alpha)$ is obtained may yield entirely different results depending on the nature of the flow field and the length of time over which the sample is obtained. If a number of these records is obtained and the PDF results are averaged, the result is

$$\overline{p(\alpha)} = \frac{1}{K} \sum_{k=1}^{K} p^k(\alpha). \qquad [3]$$

If sufficient records are used for a statistically stationary process to cover a time interval large compared with the longest significant period of fluctuation, the PDF itself becomes relatively constant. In fact, the result becomes essentially identical to a single PDF taken over a total period of time representing that used for all $K$ records.

Should the flow appear to the X-ray beam to be relatively homogeneous in the time domain, then the result of any given record will be quite similar to any other. Thus, the result due to [3] would give a low-void peak in the PDF for bubbly flow, and a high void peak due to annular-like flow. On the other hand, slug flow at one instant would appear to the X-ray beam as all water with

perhaps some entrained small bubbles and would have a PDF characteristic of bubbly flow. The next instant the major bubble would be passing the X-ray beam presenting a film on the wall and a center core free of liquid. The resulting PDF for this time slice would be similar to that of annular flow. The average of a large number of individual PDFs for this case given by [3] is expected to give a twin-peaked PDF. Summarizing, it is, then, expected that the PDF will exhibit the following behavior:

(a) Bubbly-like flows—single-peaked PDF at low void fraction.

(b) Annular-like flows—single-peaked PDF at high void fraction.

(c) Slug-like flows—twin-peaked PDF, one characteristic of bubbly flow, the other characteristic of annular flow.

It thus appears that, conceptually at least, an objective method of flow pattern determination is feasible. Of course, the preceding description presents a simplified picture and neglects some of the finer points of churn turbulent, mist annular, whispy annular, and mist flows such as described by Govier & Aziz (1972). The fine points of these flows must, of course, be analyzed separately. However, they will be expected to be a subset of the overall classification given above.

## RESULTS

It should be recalled that the necessity that bubbles smaller than the channel spacing be obtained at near atmospheric pressure required, as described in the Experimental section, that the bubbly flows be obtained in a manner different from the other flow regimes. In addition, significant developing flow effects were observed at the exit in all bubbly flow cases when even the injection ports farthest from the instrumentation sections were used. For this reason, the bubbly flow runs presented herein are not contiguous with the slug and annular flow runs in flow parameters. Thus, the flow rates of air and the void fractions reported for some bubbly flow cases are larger than the corresponding values for slug flow for the same liquid volume flux. On the other hand, all slug flow and annular data were obtained with the air injected through the channel inlet and the water injected through the porous plates 2.44 m from the exit. Lastly, the volumetric flux density of the air varies with position along the test section due to pressure drop. The values reported herein correspond to those conditions at the X-ray measuring station rather than to the channel as a whole.

### *Flow pattern observations*

There is not sufficient space available to present all the data obtained during this series of tests. For this reason, only one run in each of the three major flow regimes is presented for each of the six nominal values of liquid flux density, the nominal values being 0.0, 0.15, 0.30, 0.61, 1.52 and 3.05 m/sec. With the exception of run S52, which had a liquid flux of 2.61 m/sec, the control was within 5 per cent of nominal. Exact values are given by Jones (1973). The values of mean void fraction, centerline void fraction, and gas flux may be found in the table included with each of the data figures 3–8.

The variable nature of some regions of flow is seen in the photographs where, in some cases, more than one photograph taken within seconds of each other are shown for the same conditions. This includes most of the slug flow data. It may be noted that from the point of view of the X-rays, slug flow is a local phenomenon where there occurs the intermittent appearance of a film-core-film situation existing along the chord connecting two wetted surfaces. Thus, flattened bubbles will present this instantaneous situation when passing the X-ray beam even though their width does not approach the width of the duct. In any event, the photographs show slug flow to seldom have regular Taylor-type bubbles. Instead there frequently occurs a chaotic, twisting conglomeration of liquid and gas. The major bubbles in slug flow invariably oscillate wildly from side to side and snakewise along their length. Visual and high speed motion picture photographs show definite classical von Karman vortex street behavior by the entrained bubbles behind the

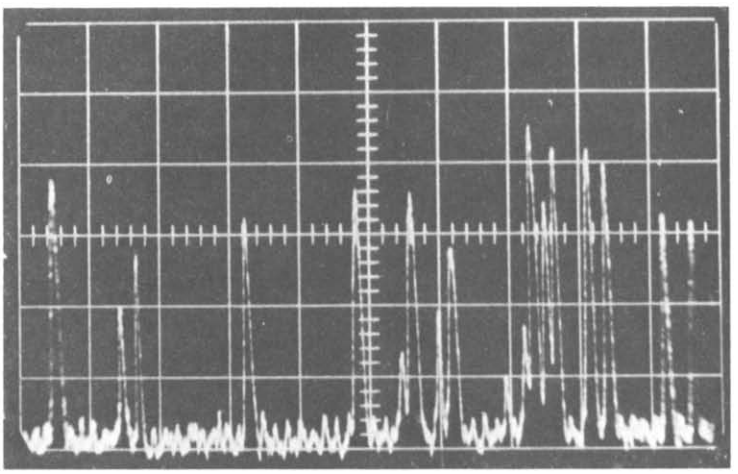

100 ms/cm

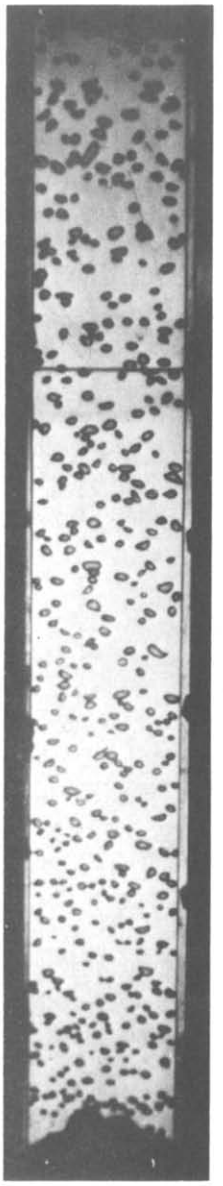

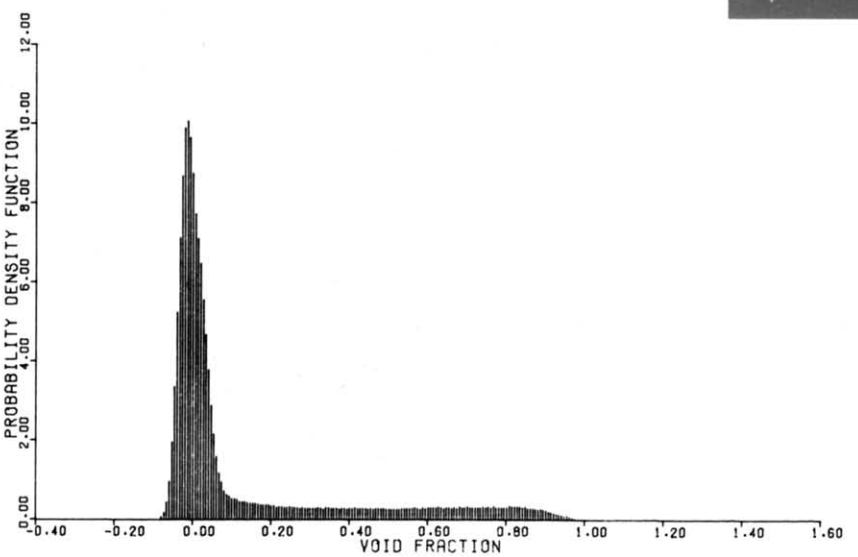


Figure 3(a).

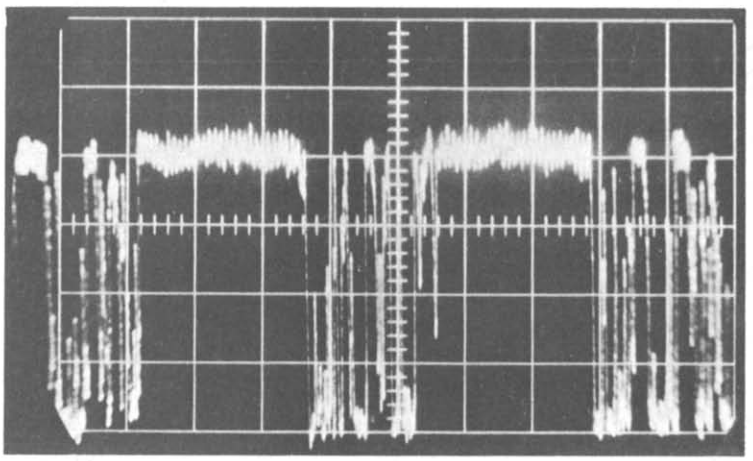

200 ms/cm

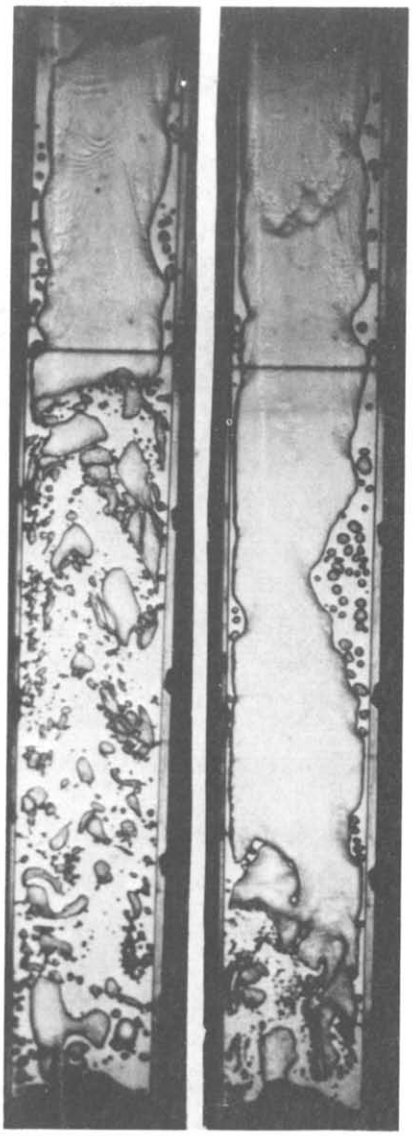

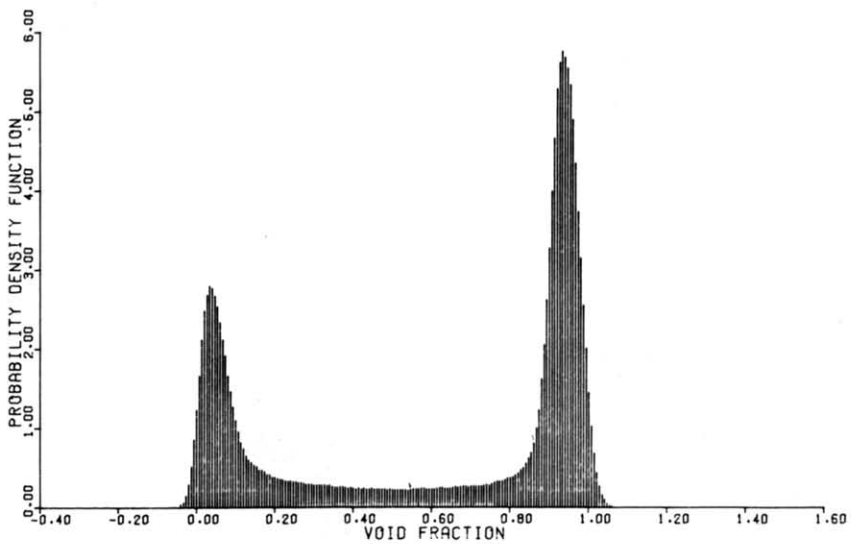


Figure 3(b).

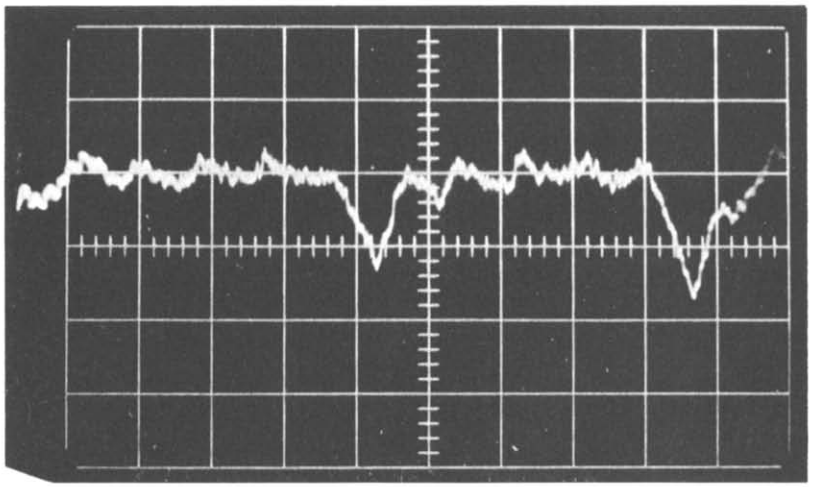

20 ms/cm

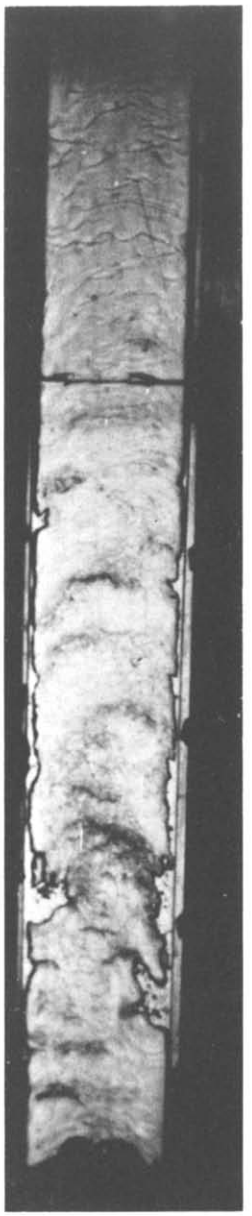

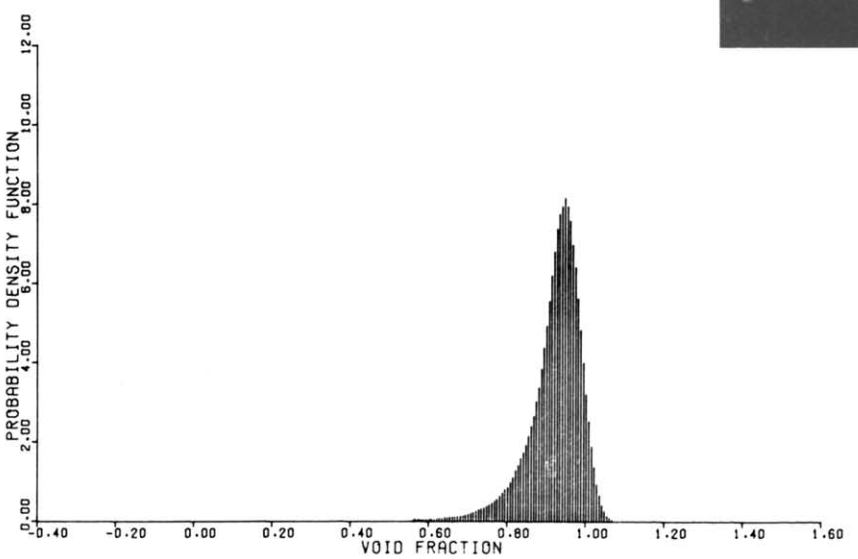


Figure 3(c).

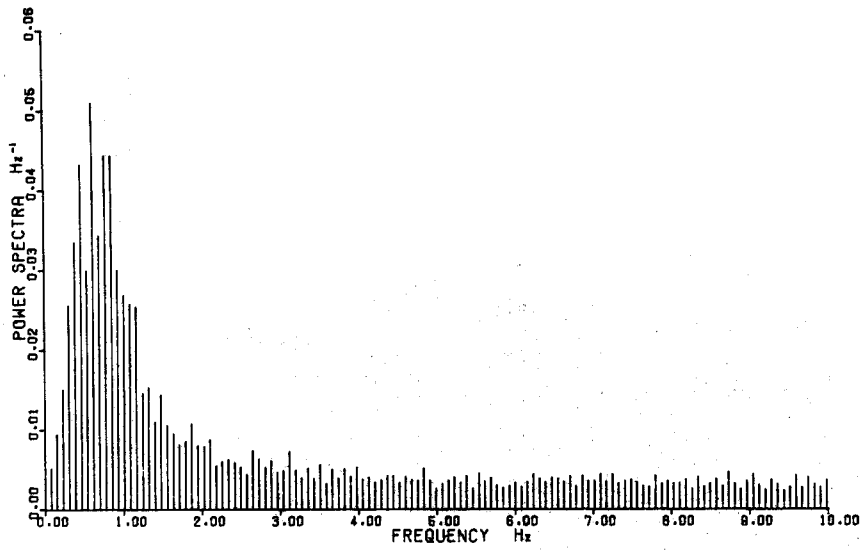


Figure 3(d).

Figure 3. Flow pattern and void oscilloscope photographs and statistical data for $j_f = 0.0$ m/s and the conditions given in the table below: (a) Bubbly flow (Run S9). (b) Slug flow (Run S4). (c) Annular flow (Run S7). (d) Average spectral density for slug flow.

| | (a) | (b) | (c) |
|---|---|---|---|
| $j_g$-m/s | 0.024 | 0.36 | 9.4 |
| $\alpha$ | 0.084 | 0.469 | 0.843 |
| $\alpha_{CL}$ | 0.128 | 0.625 | 0.920 |

major voids. Except for isolated bubbles, the nose of an elongated bubble moves, without question, sinusoidally in the transverse direction under the influence of the trailing vortex street of the preceding major void. The remainder of the bubble likewise oscillates but out of phase with the nose due to the inertial retardation of the liquid. That is, with respect to an observer situated on a packet of liquid past which a bubble is flowing, the bubble slithers lengthwise around the liquid. This tendency is seen somewhat in figure 6b, but cannot be fully appreciated without actually watching the flow.

The vortex street behavior is due to the liquid flowing past the elongated voids. Vortices are shed alternately in a manner analogous to single phase flow around a solid object. Trailing streamers are extruded from the edges of these bubbles due to liquid shear. This situation is seen in figures 4b and 7b. It is this shearing-extrusion action coupled with the subsequent breakup of these streamers that is predominantly responsible for entrained small bubbles in the liquid slugs. The size of the entrained voids is dependent on the balance of forces tending to break up the streamers and subsequently the small voids. Inertial breakup at higher liquid rates leads to the small voids shown in figures 7b and 8b while shear instability breakup results in larger voids seen in other photographs.

The bubbly flow photographs are relatively unexciting having the appearance of uniformity in all directions although some cases show the pressure reduction growth of these bubbles as they flow up the channel. Indeed, the transverse void fraction profiles presented by Jones (1973) show that bubbly flow is indeed relatively uniform over the width.

In opposition to the bubbly flow case, the annular flow photographs indicate there is not a nice smooth, two region situation existing within the test section. Both small ripples and large waves may be seen in all cases except figures 7c and 8c. These frothy "slugs" were, in fact, roll waves

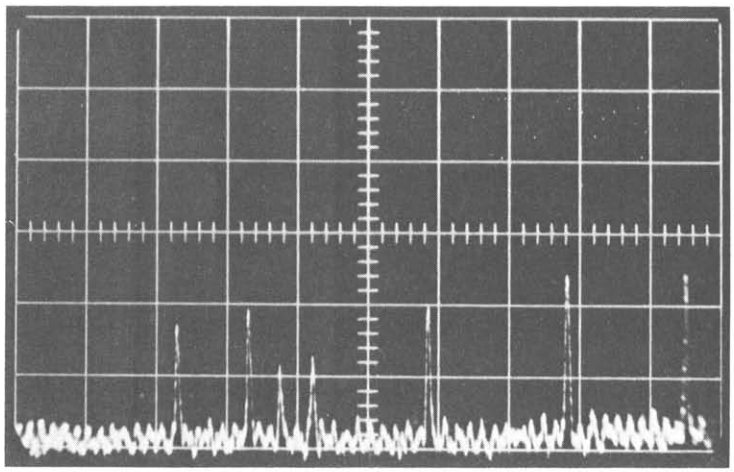

100 ms/cm

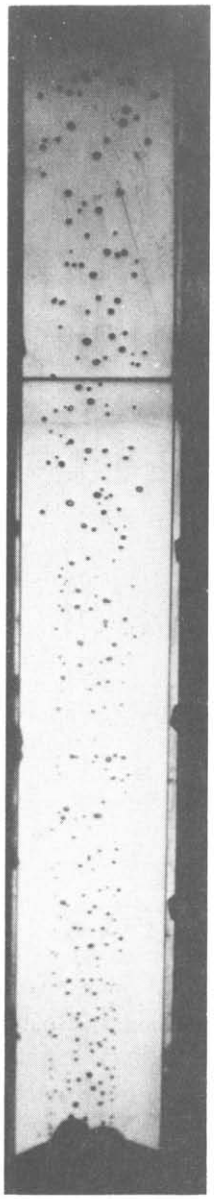

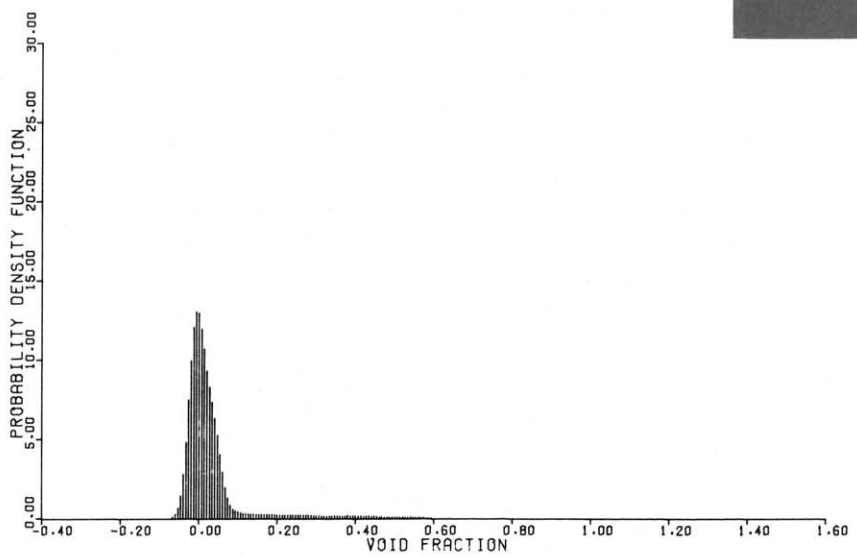


Figure 4(a).

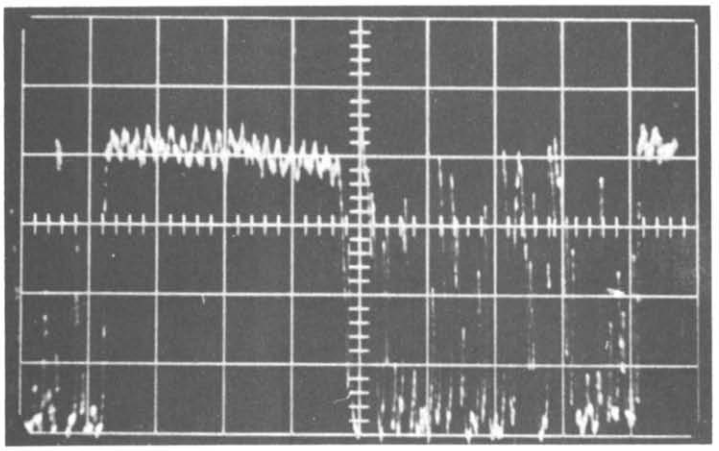

100 ms/cm

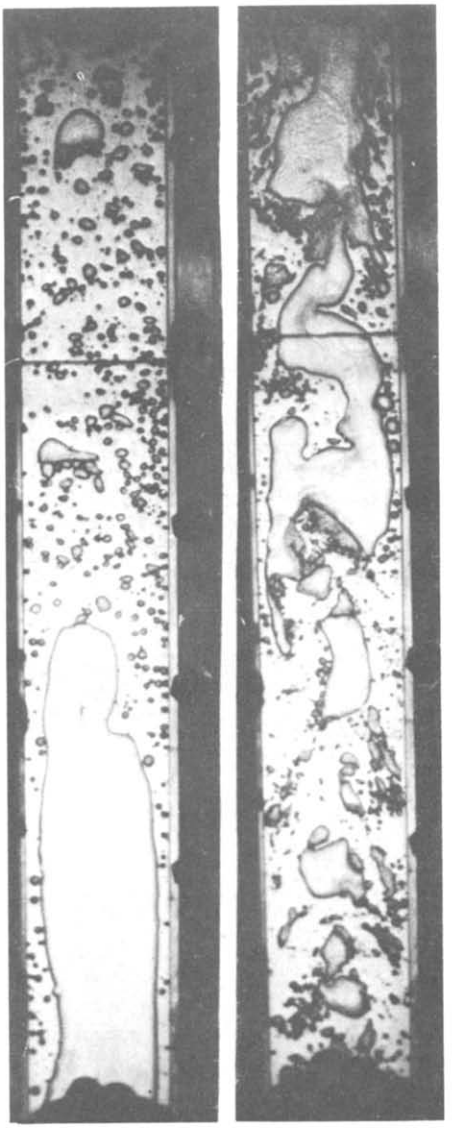

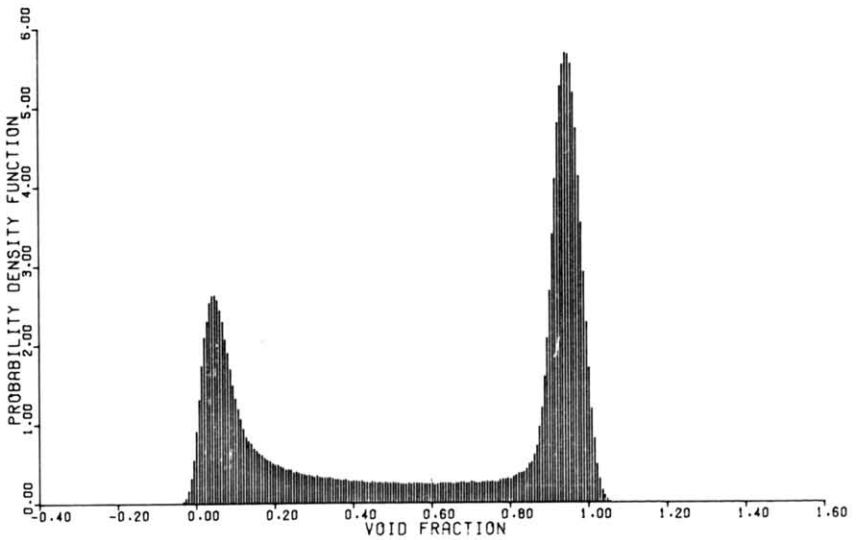


Figure 4(b).

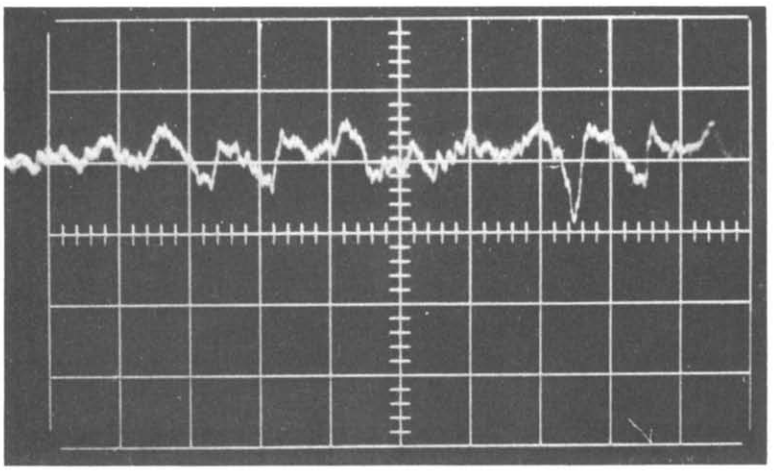

20 ms/cm

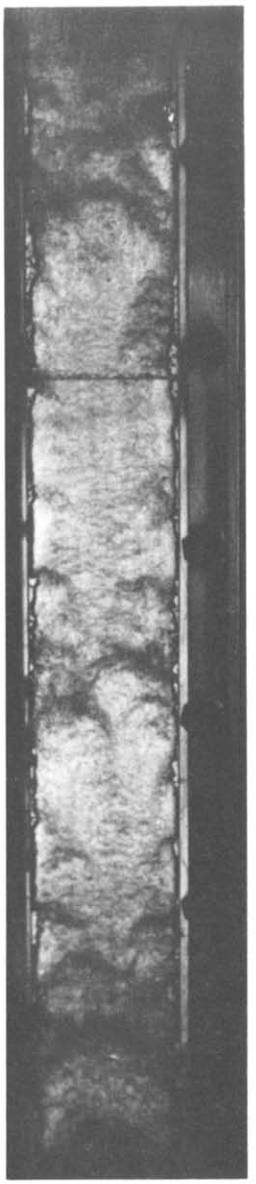

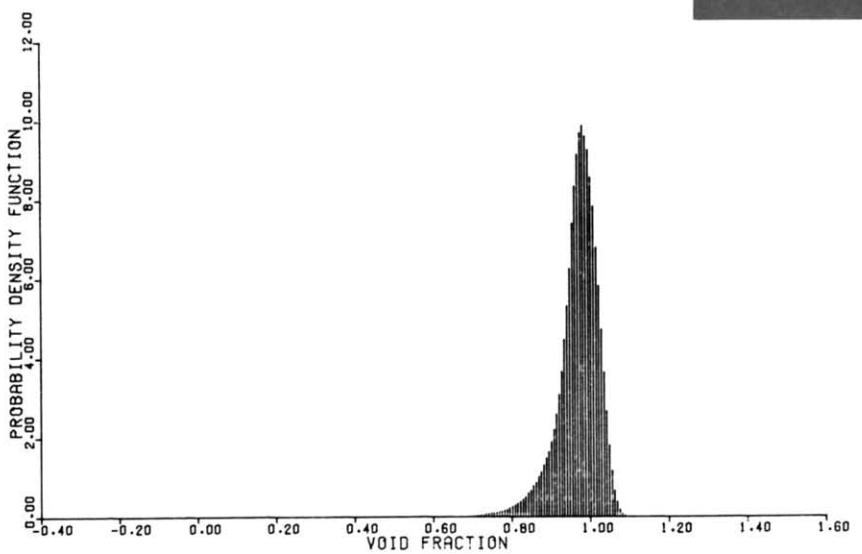


Figure 4(c).

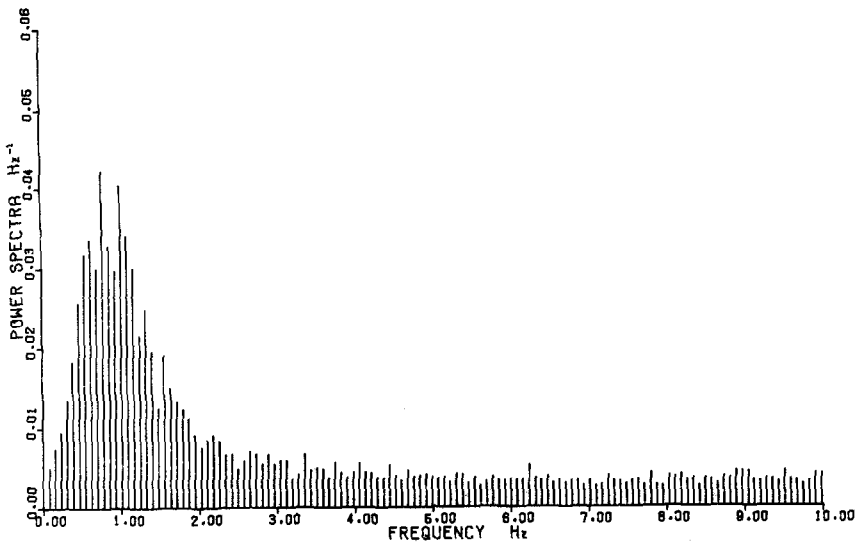


Figure 4(d).

Figure 4. Flow pattern and void oscilloscope photographs and statistical data for $j_f = 0.15$ m/s and the conditions given in the table below: (a) Bubbly flow (Run S11). (b) Slug flow (Run S15). (c) Annular flow (Run S18). (d) Average spectral density for slug flow.

| | (a) | (b) | (c) |
|---|---|---|---|
| $j_g$-m/s | 0.013 | 0.48 | 16.2 |
| $\alpha$ | 0.023 | 0.480 | 0.873 |
| $\alpha_{CL}$ | 0.035 | 0.595 | 0.981 |

which were determined by other measurements to be amorphous regions having liquid as the dispersed phase. It is suggested that these roll waves are isolated regions of high vorticity induced by the drag of the slowly moving liquid film, and the fast moving gas in the core.

In general, the distinct heterogeneous nature of the flow situations embodied in the slug flow and annular flow photographs is inescapable. The probability density data to be discussed next intensify this viewpoint and reinforce the ideas expressed in the conceptual description.

*Probability density function data*

From just an overall glance of the PDF data there seems to be finite probability that the void fraction will be outside the range of [0, 1]. This is not due to either nonlinearities in the X-ray measurement system or to nonreproducibility but is instead due to the Gaussian noise of the system itself as shown in figure 2. This noise was due to at least two sources: X-ray statistical noise inversely proportional to the photon intensity but band limited by the frequency response of the system, and also due to noise in the system electronics.

In all cases shown in figures 3–8, the transition from bubbly to slug flows is delineated by the appearance of a second maximum in the PDF at high void fractions. Likewise, the transition from slug to annular flows is marked by the disappearance of the low void, bubbly flow-like peak. There were no cases in these series of tests where this behavior was not unequivocal. Absolutely no subjectiveness was required to determine the appearance or disappearance of bridging along the X-ray measurement chord. It is felt that the probability density method presents a uniquely objective method for flow pattern determination which will allow direct comparison of results from different laboratories. In addition, there is the distinct advantage that this method may be used with nontransparent test assemblies. On this basis a quantitative definition of the occurrence

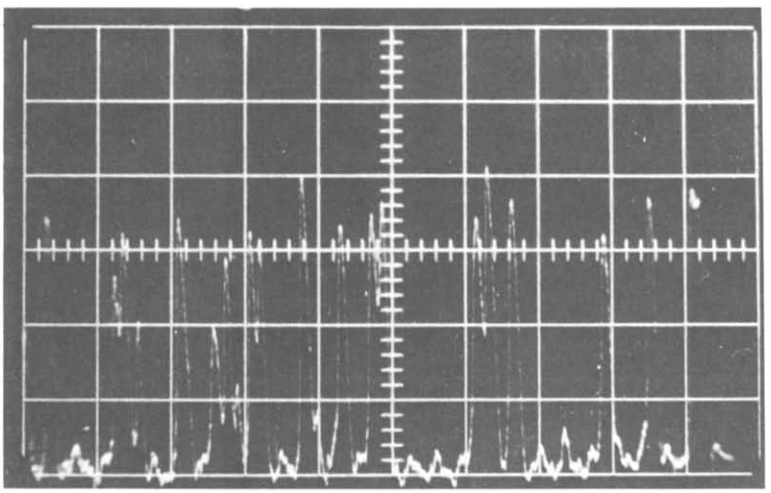

50 ms/cm

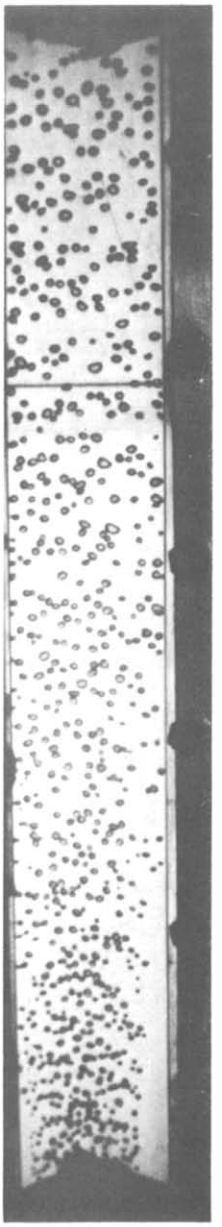

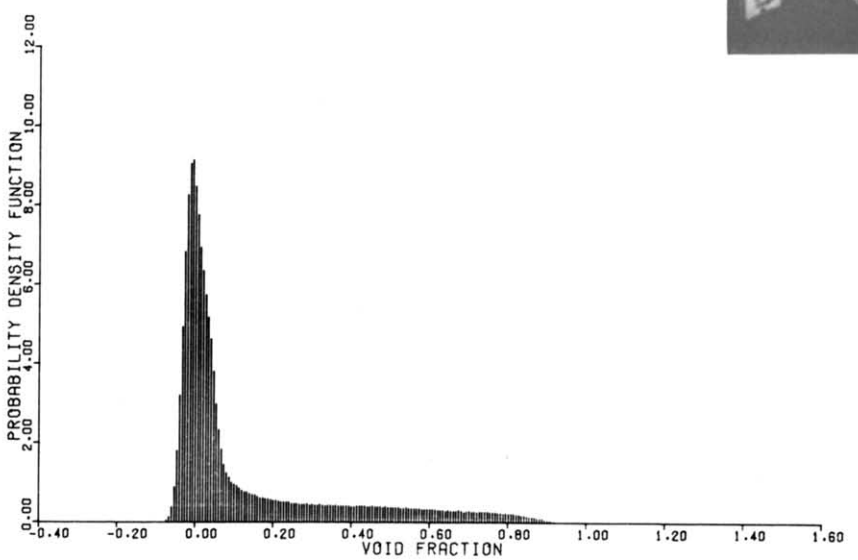


Figure 5(a)

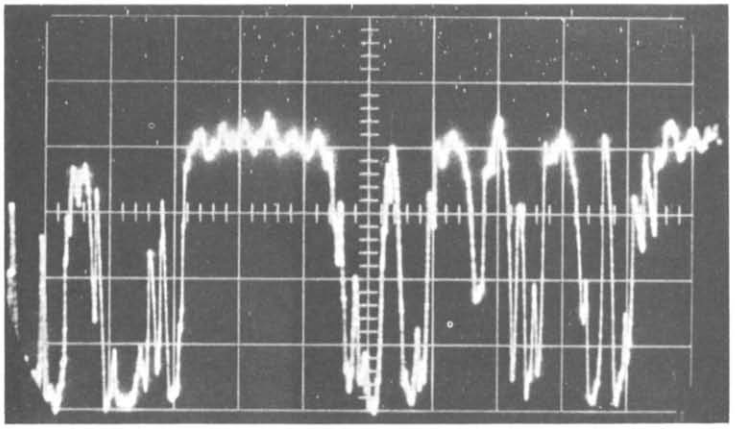

50 ms/cm

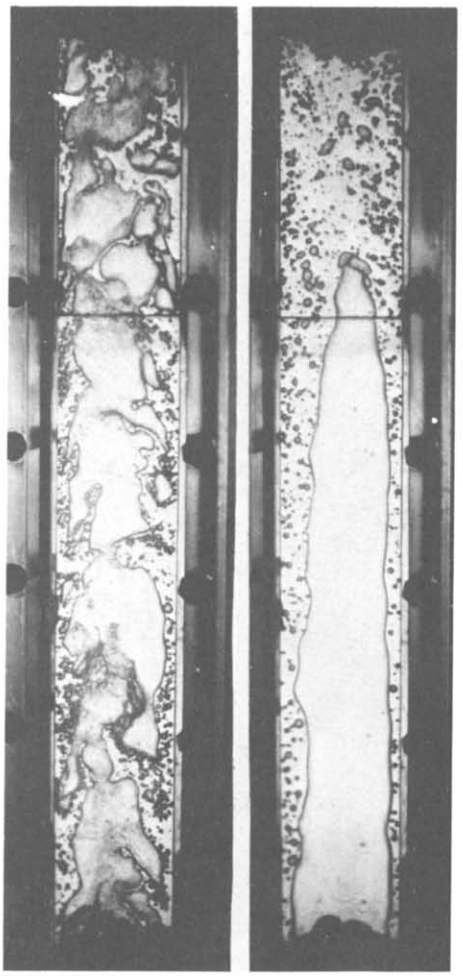

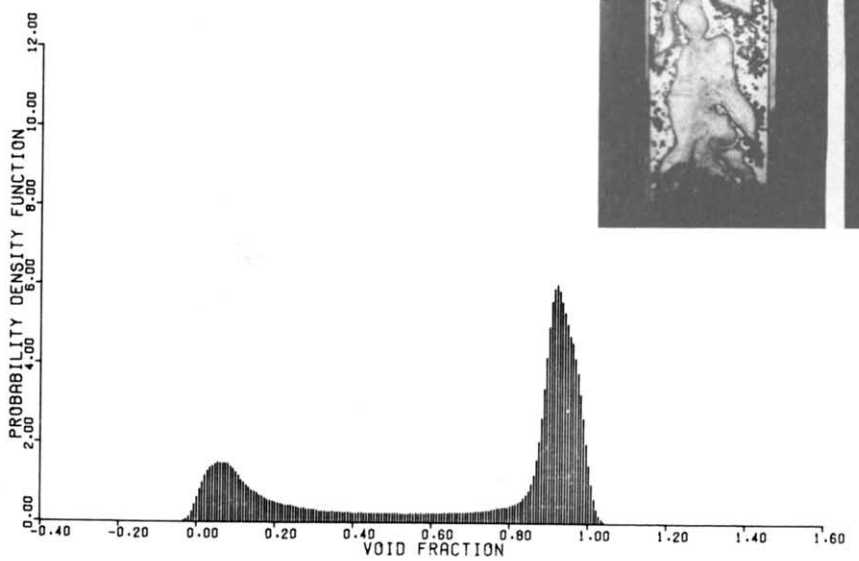


Figure 5(b).

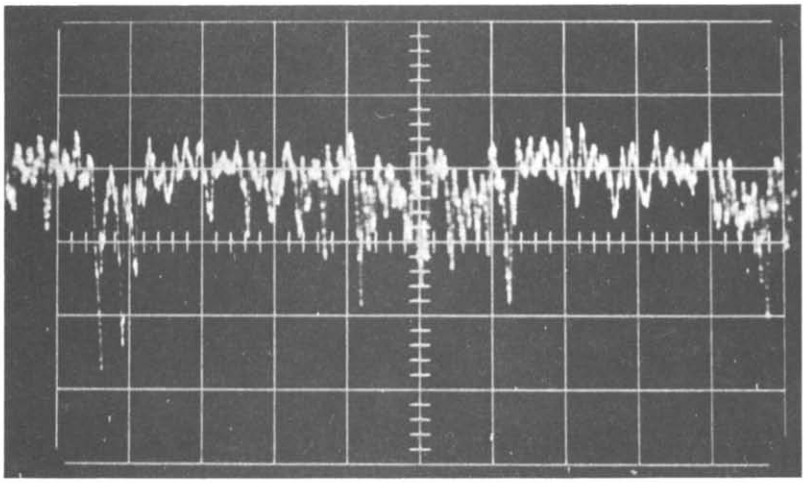

100 ms/cm

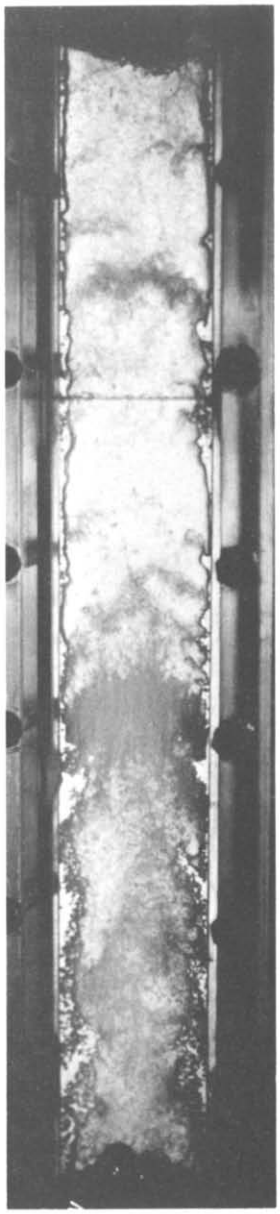

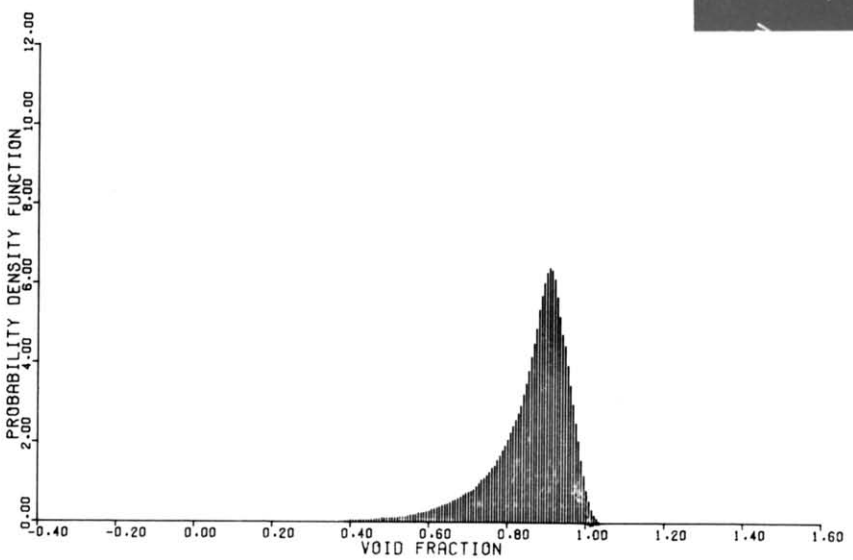


Figure 5(c).

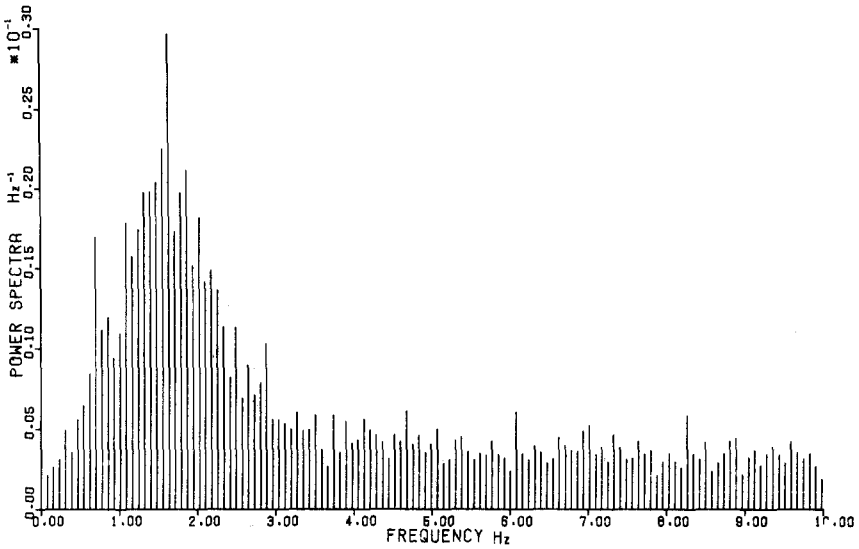


Figure 5(d).

Figure 5. Flow pattern and void oscilloscope photographs and statistical data for $j_f = 0.30$ m/s and the conditions given in the table below: (a) Bubbly flow (Run S20). (b) Slug flow (Run S22). (c) Annular flow (Run S26). (d) Average spectral density for slug flow.

| | (a) | (b) | (c) |
|---|---|---|---|
| $j_g$-m/s | 0.078 | 1.02 | 8.02 |
| $\alpha$ | 0.110 | 0.543 | 0.763 |
| $\alpha_{CL}$ | 0.131 | 0.543 | 0.822 |

of slug flow between two wetted surfaces would be:

> Slug-like flow is that localized condition characterized by the appearance of two separate and statistically significant localized maxima in the probability density function of chordal void fluctuations as measured by a transient X-ray void photometer.

The two key phrases are "localized condition," and "statistically significant." Slug flow could exist at one point in, say, a rod bundle, while annular flow or subcooled bubbly flow could exist in another region. In order to be statistically significant, the maximum involved must be clearly existent when taken in consideration of the local measurement irregularities of the probability density function. Bubbly and annular flows, on the other hand would simply be determined by the non-occurrence of slug flow coupled with the appropriate void fraction. The results of this definition for the data are shown in figure 9. Except for the $j_f = 0$ m/s data, transition from bubbly to slug flow occurs near 20 per cent void fraction while transition from slug to annular flow occurs near 80 per cent void fraction.

Examination of the PDF data reveals another characteristic which yields important ideas regarding the structure of two-phase flow. If the low-void half of the PDF is examined, it is difficult to determine the difference between this and a typical bubbly flow situation. Similarly for the high-void half, it looks and behaves quite like annular flow. On this basis it is suggested that slug flow may be treated as a transition flow which occurs as a periodic time combination of bubbly and annular-like flows. It would seem that this suggestion is quite remarkable in that this transition in some cases would span over 60 per cent of the void fraction range from less than 20 per cent to over 80 per cent voids. That the combination is periodic shall be discussed in the next section regarding power spectral densities.

There are considerable other pieces of information obtainable from the PDF data including

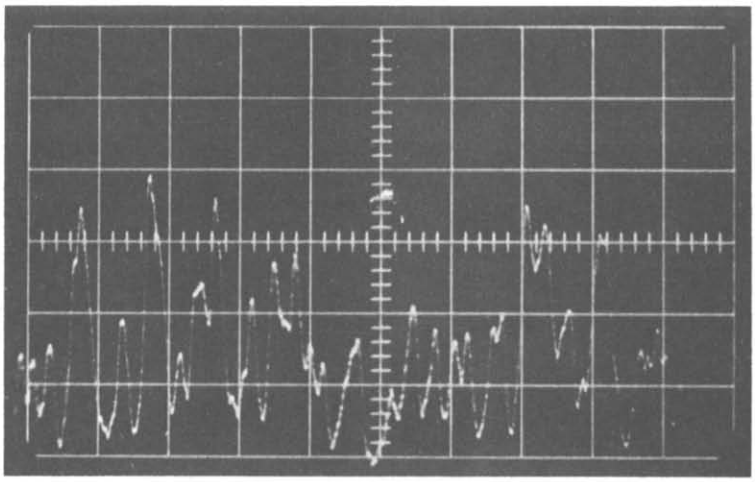

20 ms/cm

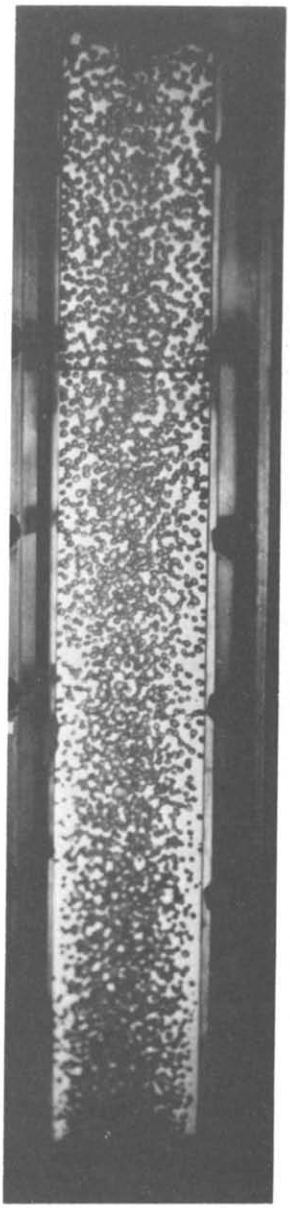

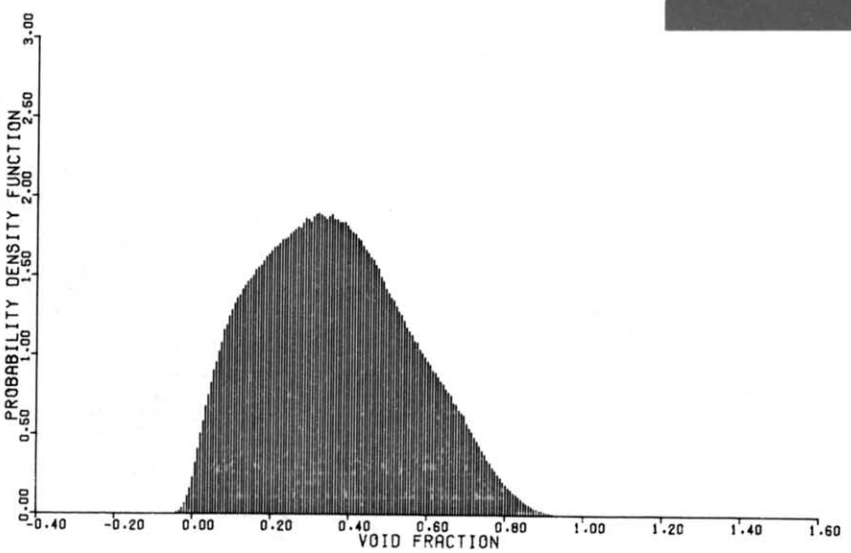


Figure 6(a).

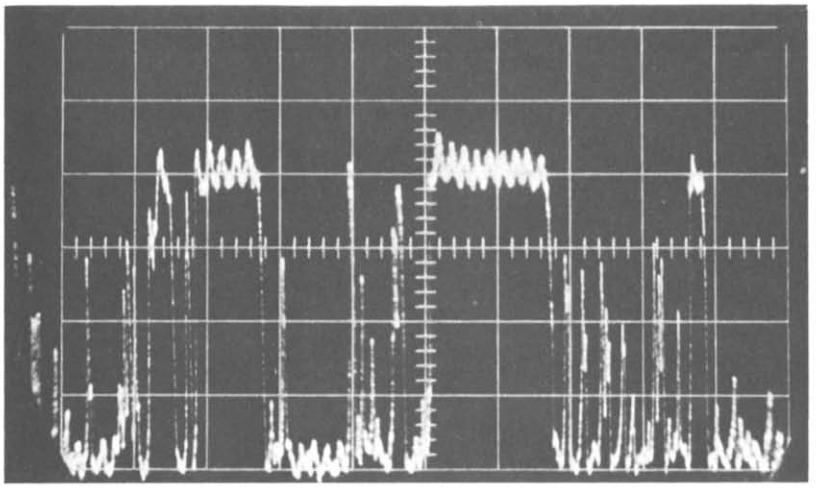

100 ms/cm

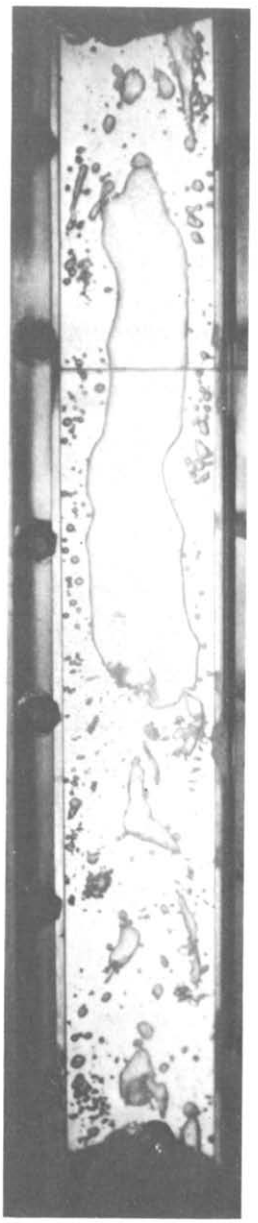

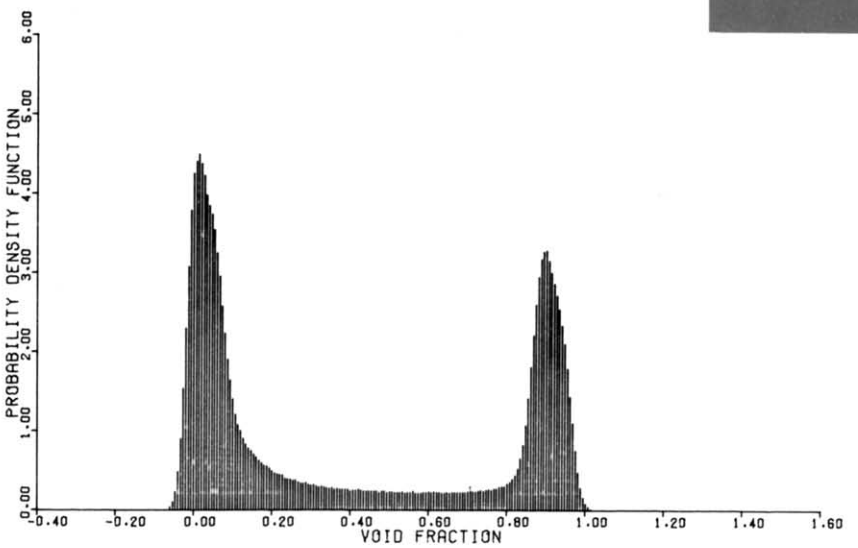


Figure 6(b).

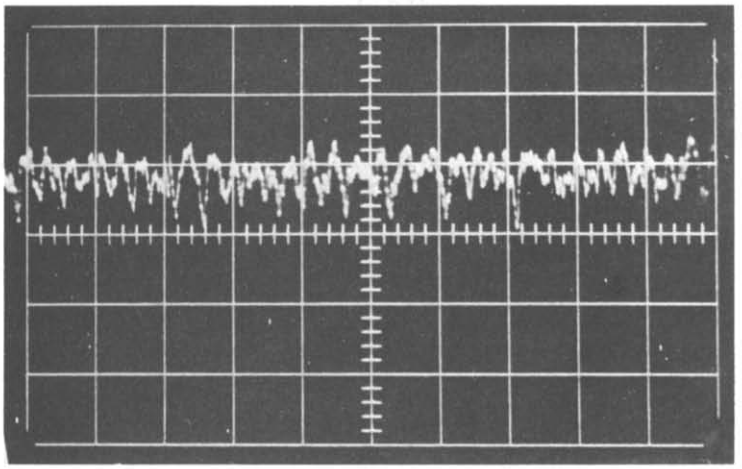

50 ms/cm

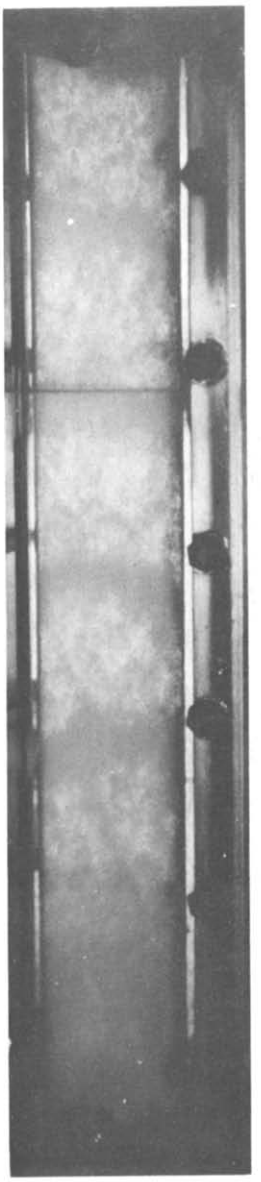

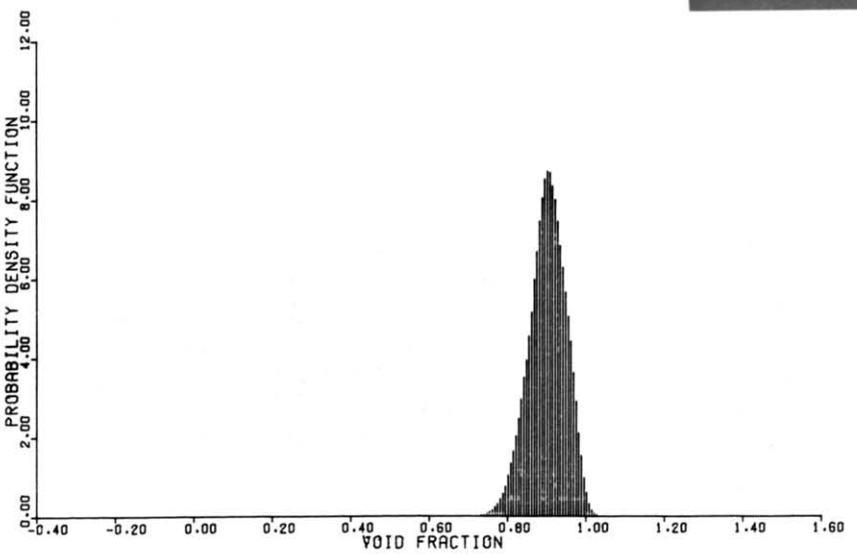


Figure 6(c).

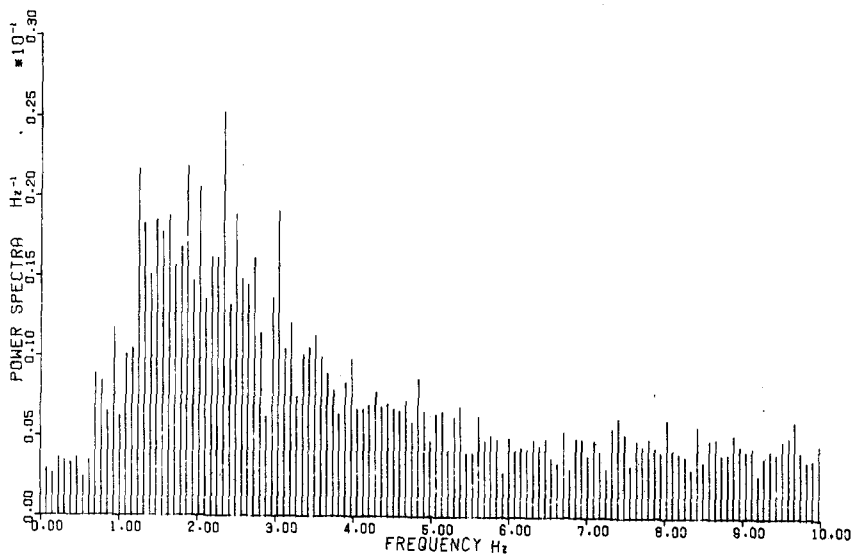


Figure 6(d).

Figure 6. Flow pattern and void oscilloscope photographs and statistical data for $j_f = 6.1$ m/s and the conditions given in the table below: (a) Bubbly flow (Run S32). (b) Slug flow (Run S34). (c) Annular flow (Run S38). (d) Average spectral density for slug flow.

| | (a) | (b) | (c) |
|---|---|---|---|
| $j_g$-m/s | 0.38 | 0.40 | 33.1 |
| $\alpha$ | 0.392 | 0.251 | 0.886 |
| $\alpha_{CL}$ | 0.373 | 0.413 | 0.912 |

film thickness, void fraction in the slugs in slug flow, slug residence time fractions, and slug and bubble lengths. Some of these are described below.

*Film thicknesses.* Considering the ideas expressed in the thought experiment, and the fact that the system noise was Gaussian as shown in figure 2, the point at which the maximum occurs in the annular flow PDF represents the most probable void fraction. Assuming there to be negligible quantities of liquid in the gas core this void fraction would represent the film thickness. This assumption was verified by other measurements. Likewise in slug flow the maximum void fraction at which this local maximum in the PDF occurs could also represent the film thickness adjacent to the major bubbles. Mathematically if $\delta_s$ represents the film thickness on the wall perpendicular to the small dimension spacing $s$, this may be represented by

$$\max\{\alpha|_{\max p(\alpha)}\} = \left(1 - \frac{2\delta_s}{s}\right). \qquad [4]$$

Film thicknesses so calculated for all slug and annular flow data are shown in figure 10. In general there does not appear to be much which separates the slug flow data from that obtained for annular flow. In both cases if the liquid inertia effects are small, the dynamics are governed by a balance between shear and gravity forces. The limiting film thicknesses measured for vanishing liquid flow rates appear to be clustered about the value of 0.045 given by Wallis & Collier (1968) for viscosity numbers

$$N_v = \left\{\frac{gd^3\rho_f\Delta\rho}{\mu_f^2}\right\}^{1/2} \qquad [5]$$

of about 2800. Here $g$ is the acceleration of gravity, $d$ is the characteristic dimension, $\rho_f$ and $\mu_f$

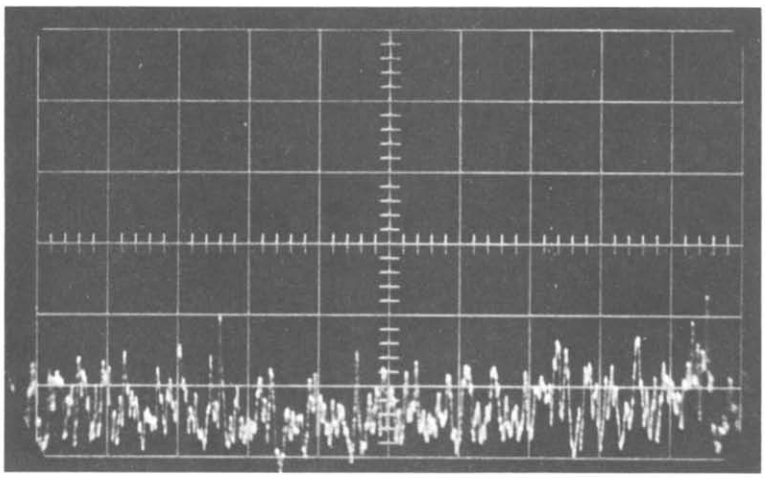

50 ms/cm

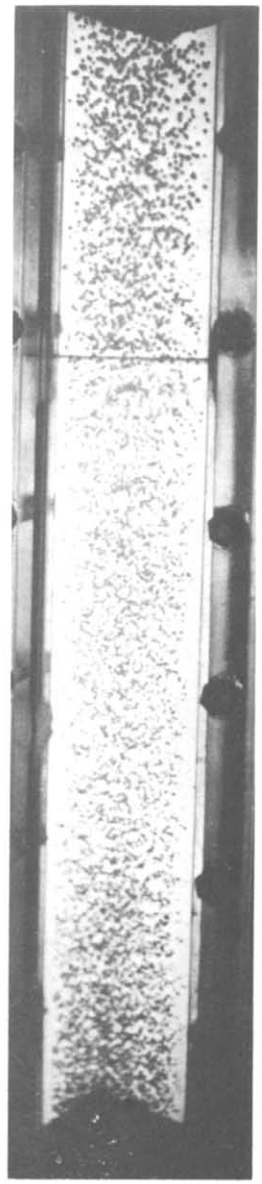

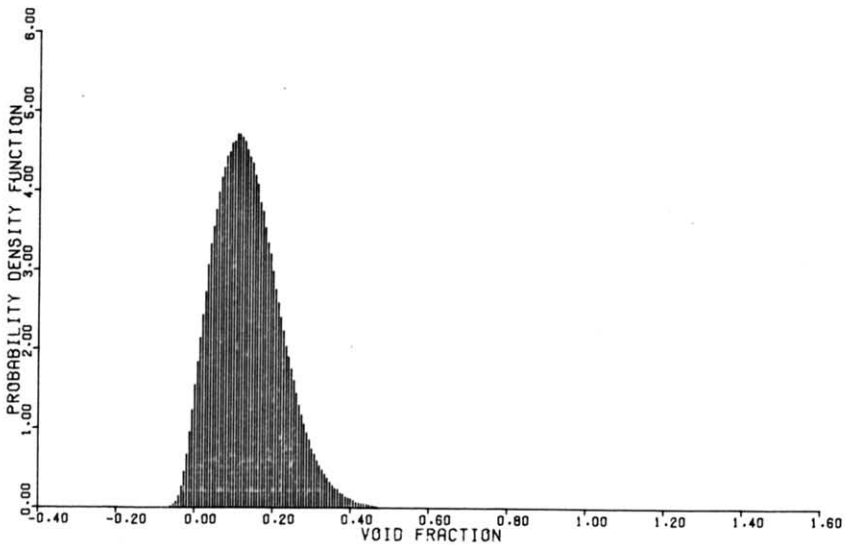


Figure 7(a).

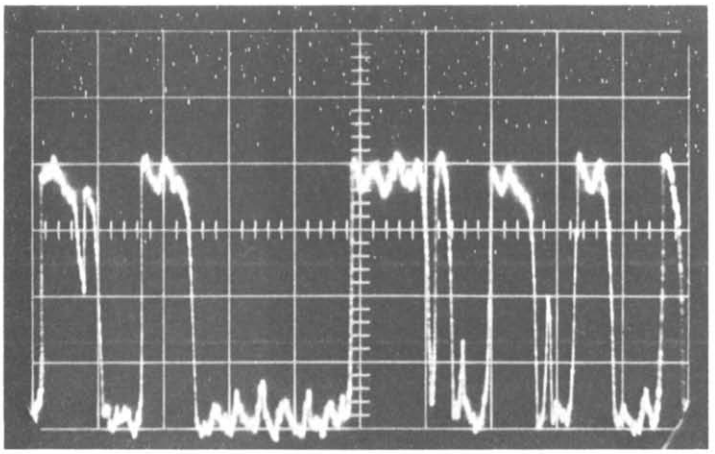

50 ms/cm

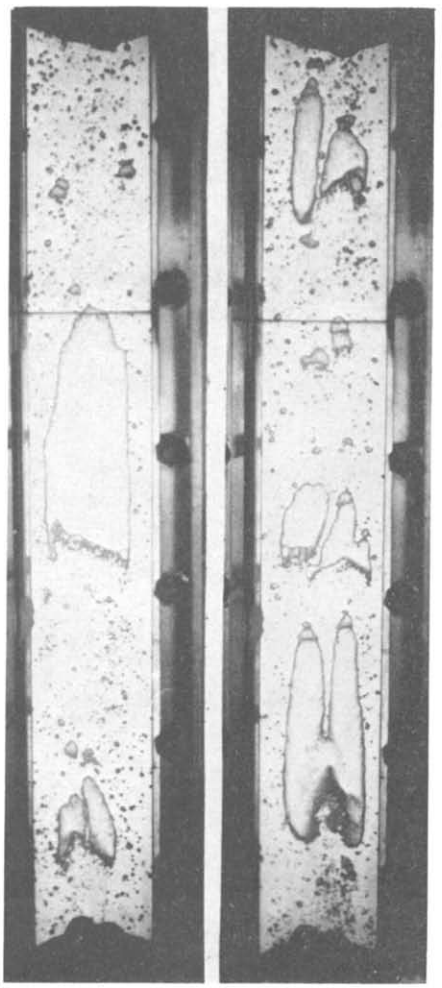

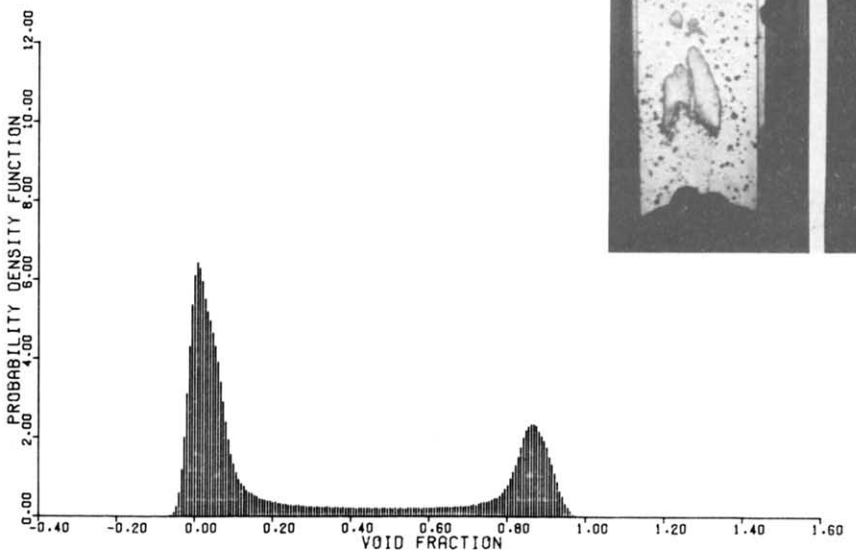


Figure 7(b).

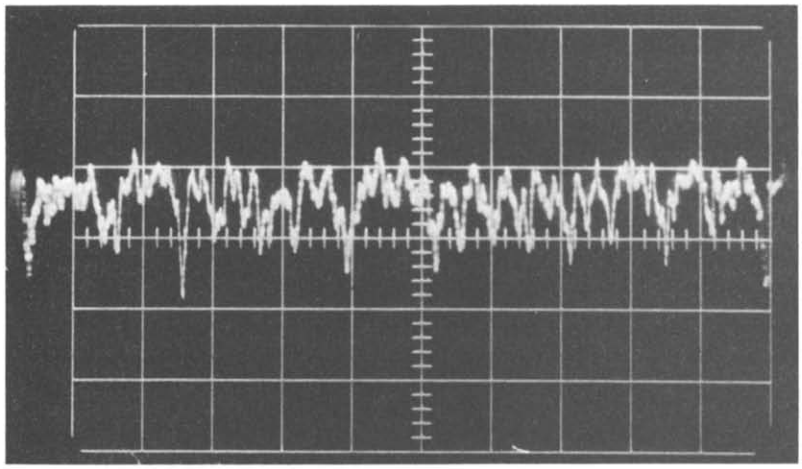

50 ms/cm

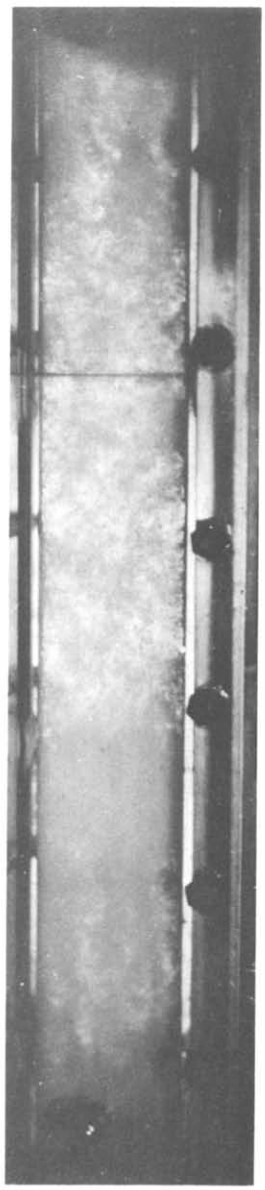

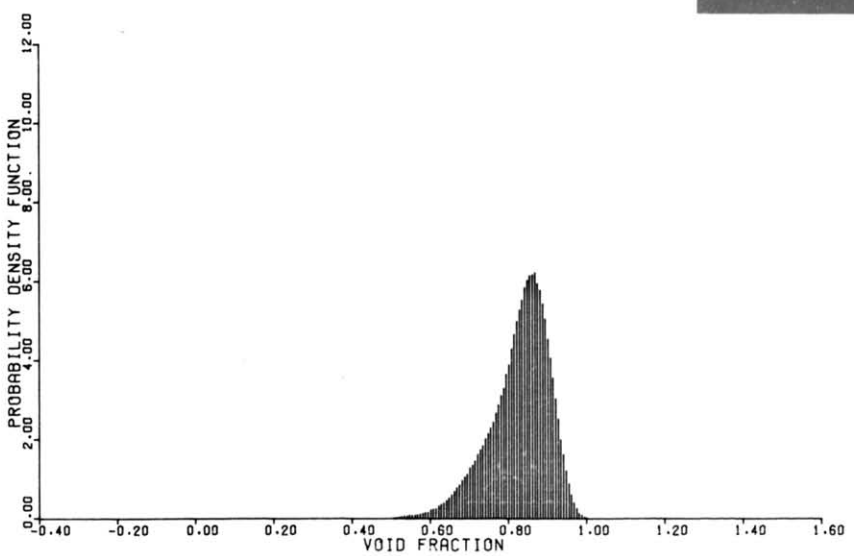


Figure 7(c).

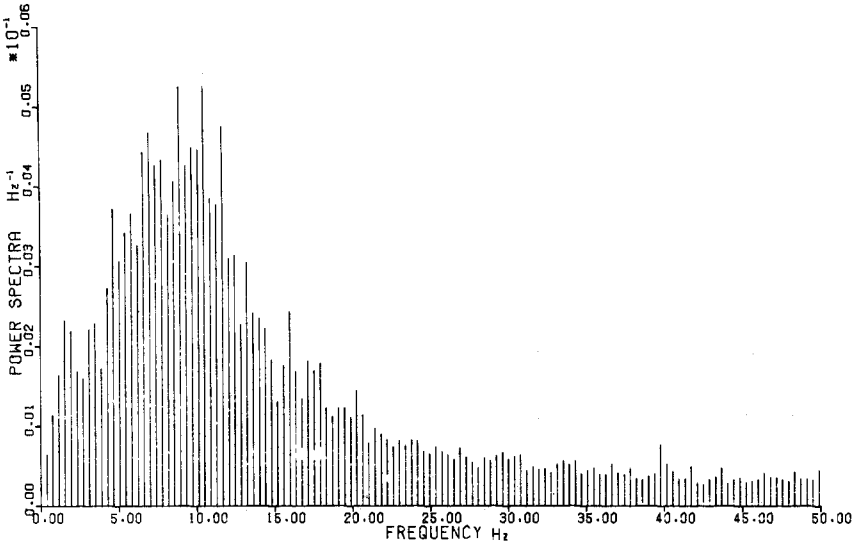


Figure 7(d).

Figure 7. Flow pattern and void oscilloscope photographs and statistical data for $j_f = 1.52$ m/s and the conditions given in the table below: (a) Bubbly flow (Run S40). (b) Slug flow (Run S42). (c) Annular flow (Run S46). (d) Average spectral density for slug flow.

| | (a) | (b) | (c) |
|---|---|---|---|
| $j_g$-m/s | 0.196 | 0.503 | 23.4 |
| $\alpha$ | 0.083 | 0.168 | 0.814 |
| $\alpha_{CL}$ | 0.140 | 0·317 | 0.836 |

are density and viscosity of the saturated liquid respectively while $\Delta\rho$ is the vapor–liquid density difference.

*Slug residence times.* The probability density functions can, as discussed previously, be thought to be made up of a number of individual PDFs, averaged over a long time compared with the longest period of concern in the flow field. On this basis it can be shown that the ratio of slug residence time to bubble residence time is

$$\frac{t_s}{t_b} = \frac{p_{\max}(\alpha_s)}{p_{\max}(\alpha_b)} \qquad [6]$$

which is true in the ideal case where the noise is constant and where there is no probability that any void fractions exist except those at $\alpha_s$ and $\alpha_b$.

The slug residence time fractions may be calculated from [6] with a small correction for variation in standard deviation with void fraction with the results shown in figure 11. It is notable that all data are correlated by a single line. The two points at void fractions less than 20 per cent are for classical, cylindrical, cap-type flows, where extremely quiescent, low gas flow bubbled up through a static liquid column. Extrapolation of the slug time fraction to zero indicates transition from slug to annular flow occurs for all flow conditions near 80 per cent. This agrees well with the observations of other investigators using circular ducts. It therefore appears that the dynamics which cause the final disappearance of liquid bridging in round tubes at the transition to annular flow are similar to those which exist at the centerline of a rectangular duct when the first indications that transition to annular flow exist. The reader is reminded, however, that the void fractions used in this figure are centerline void fractions and not cross section average values. For the test conditions given by Jones (1973) which included the liquid and gas volume flux ranges of

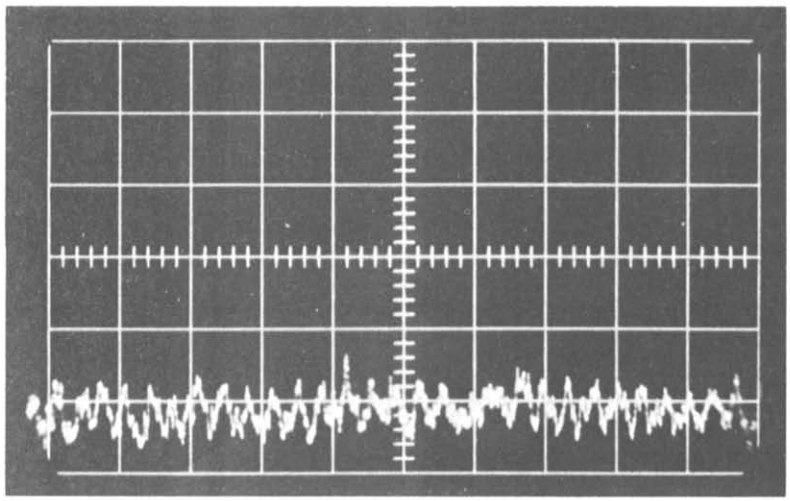

50 ms/cm

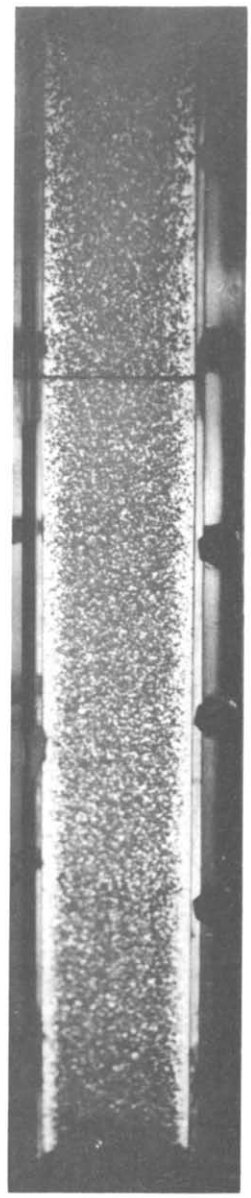

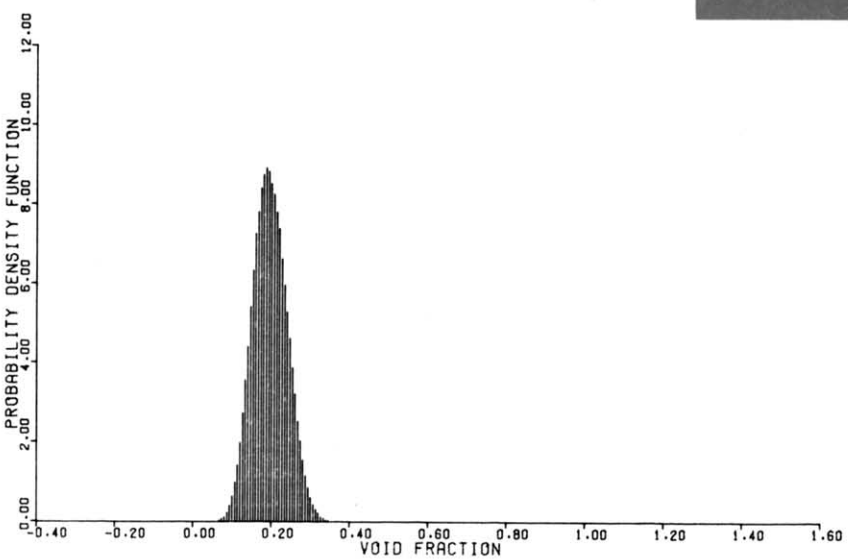


Figure 8(a).

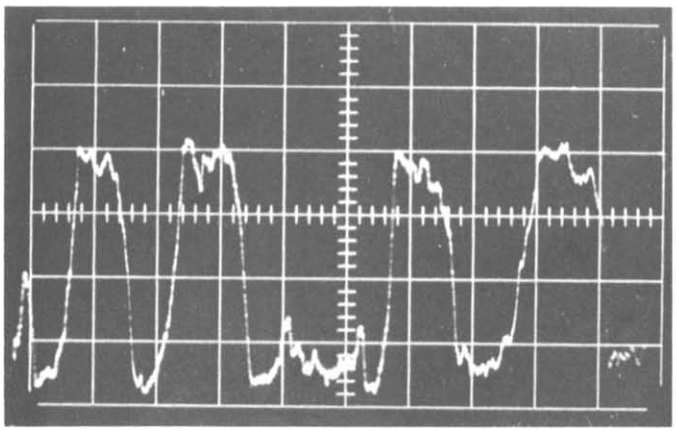

20 ms/cm

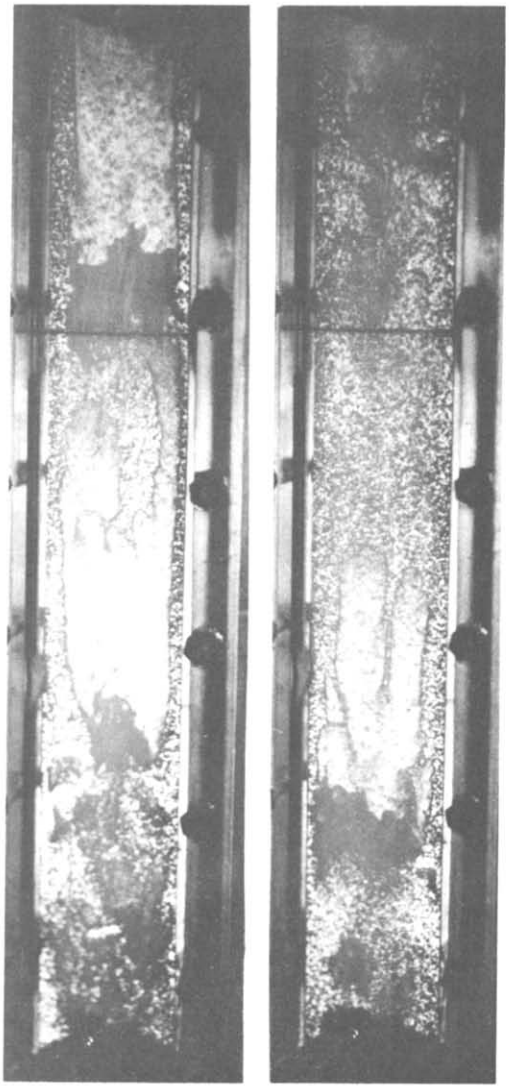

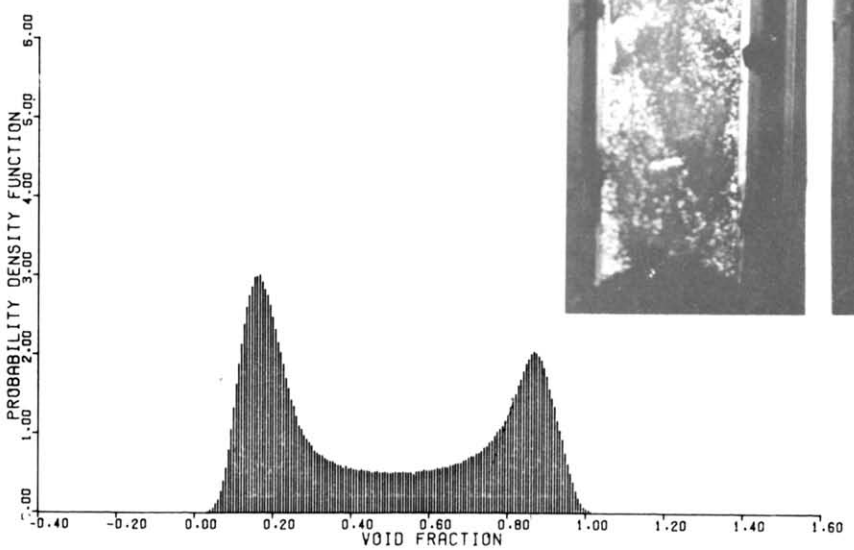


Figure 8(b).

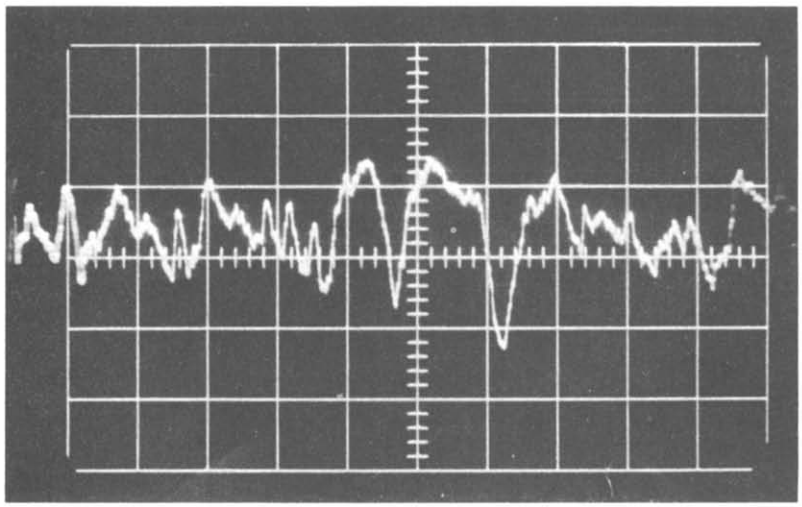

20 ms/cm

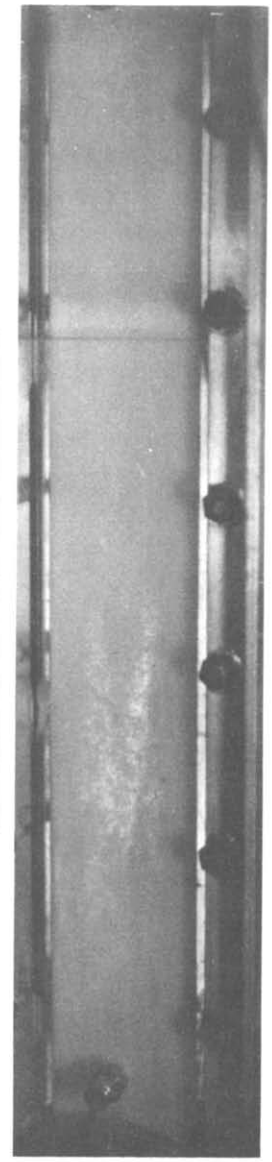

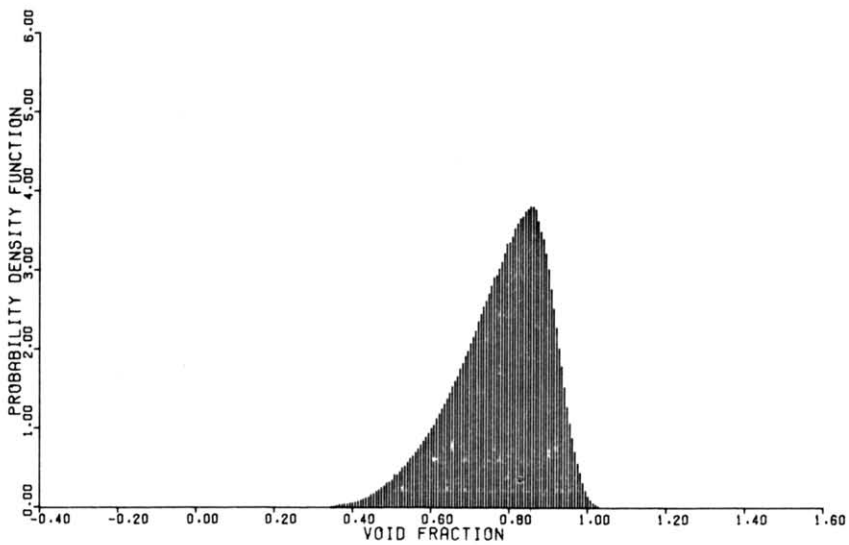


Figure 8(c).

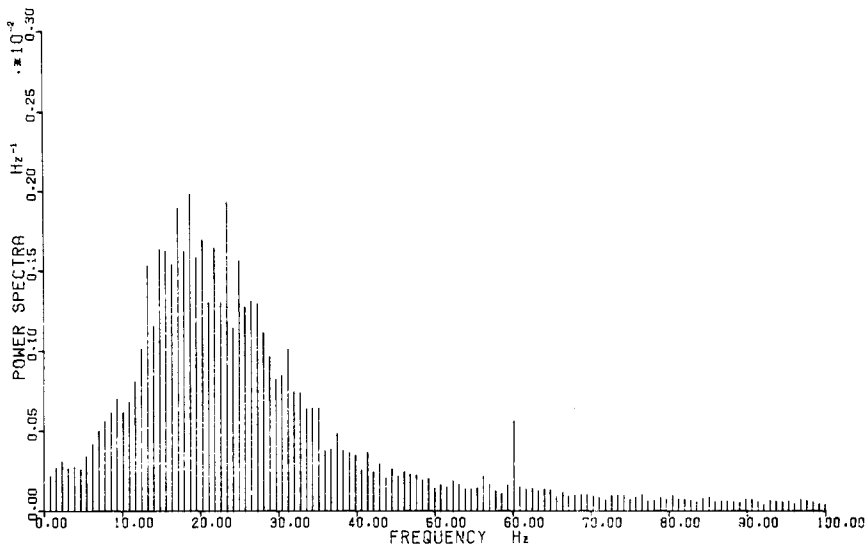


Figure 8(d).

Figure 8. Flow pattern and void oscilloscope photographs and statistical data for $j_f = 3.04$ m/s and the conditions given in the table below: (a) Bubbly flow (Run S48). (b) Slug flow (Run S50). (c) Annular flow (Run S52). (d) Average spectral density for slug flow.

| | (a) | (b) | (c) |
|---|---|---|---|
| $j_g$-m/s | 0.65 | 2.32 | 17.1 |
| $\alpha$ | 0.142 | 0.341 | 0.739 |
| $\alpha_{CL}$ | 0.194 | 0.468 | 0.786 |

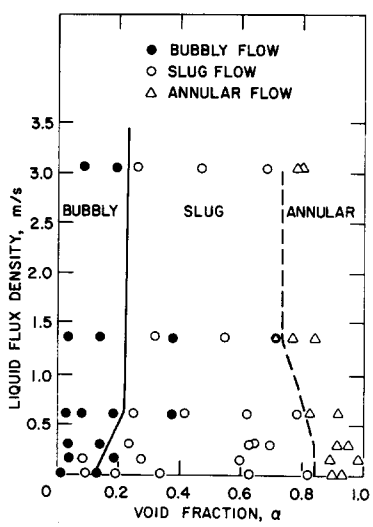


Figure 9. Flow pattern map based on PDF determination.

$0 \leq j_f \leq 3.05$ m/sec, and $0 \leq j_g \leq 34$ m/sec, the ratio of centerline void fractions to mean void fraction covered the range given in table 1.

*Power spectral densities.* The work previously presented provides for determining the local flow pattern on an objective basis, shows how to determine the film thicknesses in slug and annular flows, and indicates how to obtain the slug residence time ratio in slug flow. Knowing this ratio, however, does not provide sufficient information to synthesize all modes since there is an infinite combination of lengths and velocities which would all give the same ratio. Now in slug

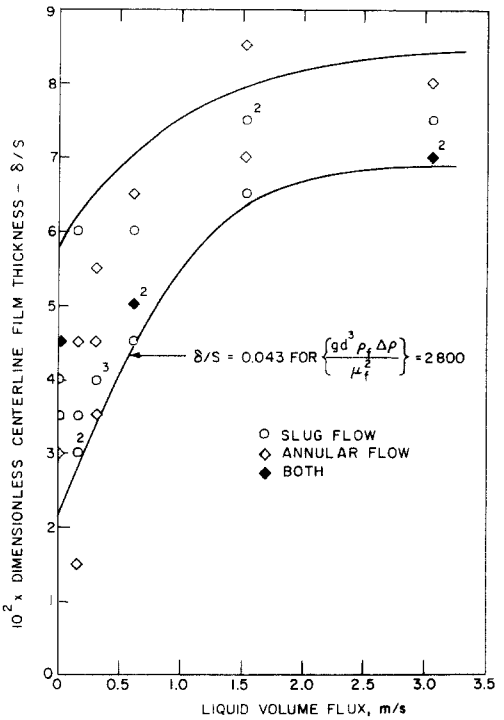


Figure 10. Dimensionless film thickness as obtained from the PDF data.

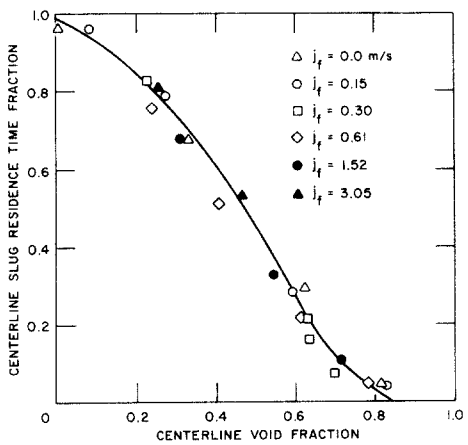


Figure 11. Correlation of slug residence time fraction by the channel centerline void fraction.

Table 1. Range of centerline-mean void fraction ratios for the three major flow regimes

| Flow patterns | Ratios |
|---|---|
| Annular flow | 1.01–1.23 |
| Slug flow | 1.18–2.00 |
| Bubbly flow | 1.11–1.79 |

flow, there is no relative velocity between the bubbles and the slugs. Even with relative velocity between the gas and the liquid, the slugs move at the bubble velocity. This is because as the liquid in a slug drains around the trailing bubble it is made up by the liquid which drains around the preceding bubble. The slugs are not fixed masses but, in steady-state slug flow are volumes moving with a velocity equal to that of the major bubbles, and through which liquid continually passes. It can be easily shown that the bubble and slug lengths, $L_s$ and $L_b$, can be calculated by a

cell model to give

$$L_b = \frac{j_g}{\alpha f}\left\{\frac{1}{1+t_s/t_b}\right\}; \quad L_s = \frac{j_g}{\alpha f}\left\{\frac{1}{1+t_b/t_s}\right\} \qquad [7]$$

where $f$ is the characteristic slug frequency and $t_s$ and $t_b$ are the average slug and bubble residence times. Thus if the residence time ratio is found from the PDF by [6] and the dominant frequencies are determined, then the cell lengths may be obtained from [7].

The method used in the data presented herein was to obtain the time averaged spectral density (PSD) of the void fraction signal by complex multiplication of the Fourier transform of each record by its conjugate. Thus, if

$$F_\alpha(\omega) = \int_{-\infty}^{\infty} \alpha(t)e^{-j\omega t}\, dt \qquad [8]$$

where $\omega$ is a characteristic frequency and where $\alpha(t)$ is truncated in $(-T, T)$, the spectral density is calculated directly by

$$S_\alpha(\omega) = \frac{1}{T} F_\alpha(\omega)F_\alpha^*(\omega) \qquad [9]$$

where the asterisk denotes the conjugate. Obtaining the spectral density of the fluctuations has an additional advantage in that it will show where periodicities exist in the signal to the extent they can be resolved from the noise spectrum inherent in the system.

The results for each of the slug flow runs is included in the "$d$" portion of each of figures 3–8. There is no doubt of the strong periodicities in this flow pattern, although the spectra are apparently continuous rather than discrete. If the dominant frequencies are taken to be those where the maximum in the PDS occurs, then the results of all the data are as shown in figure 12.

*Slug lengths and residence times.* The slug residence time ratios were calculated from [6] with the results shown in figure 10. Using the residence time ratios, the slug lengths were calculated from [7] and are presented in figure 13. There also appears that the data would be reasonably well correlated by a single line. This behavior is expected since the slug length would vanish as

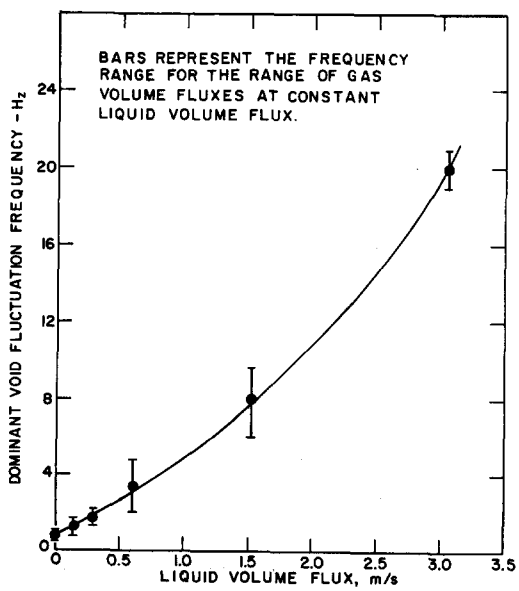


Figure 12. Dominant void fluctuation frequencies in slug flow determined from the spectral density.

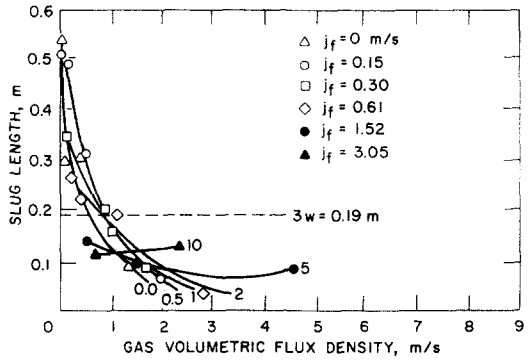


Figure 13. Slug length as determined from centerline void fractions, PDF, and PSD data.

transition to annular flow occurs. Using the ideas of Moissis (1962) an order of magnitude estimation of the slug length may be obtained as $L_s = 0(3w)$. This value is shown on figure 13.

*Fluctuation frequency of bubbly and annular flows.* The maximum magnitude of the fluctuations in slug flow is larger than those of either bubbly flow or annular flow, and strong periodicities appear. Alternatively, the void fluctuations in bubbly flow appear completely random with no periodicity. In the latter case the PSD's were flat indicating a completely random nature. Apparently any periodicity due to generation of bubbles at porosity locations in the air-injection ports is wiped out by the turbulent fluctuations in the carrier fluid. This is in agreement with the results of Lackme (1964).

For annular flow the periodicities were not at all as definite as those shown for slug flow, and amounted to a small percentage of void fraction. In all cases the power per unit frequency in all frequency intervals was less than that of the 60 Hz system noise. The results of the PSD data for annular flow are shown in figure 14. It is felt that these are the frequencies of the frothy slugs, or roll waves, traveling down the channel since these frequencies correspond with those observed by Hewitt & Lovegrove (1969).

## DISCUSSION AND CONCLUSIONS

It has been shown that considerable fundamental information regarding the structure of two-phase flows may be obtained from the statistical behavior of the void fraction. In fact Akagawa (1971) has shown a direct correlation between void and pressure drop fluctuations in two-phase flows. It is suggested that the classification of two-phase flows in vertical ducts be

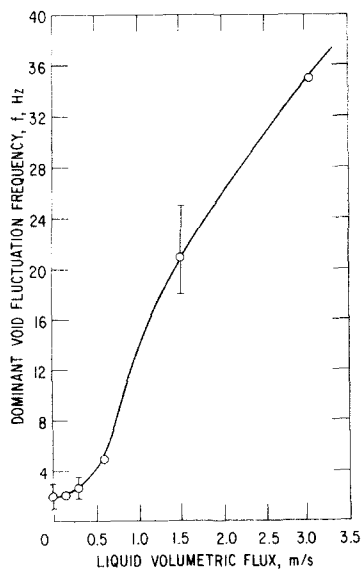


Figure 14. Void fluctuation frequencies in annular flow.

structured such that there would be three dominant patterns according to their gross behavior and our herein demonstrated ability to objectively determine their existence in opaque geometries. These dominant regimes would consist of the bubbly, slug and annular regimes. Subsets of these would include the isolated bubble regimes, churn turbulent and frothy flows, and whispy and mist annular flows. Completely dispersed mist flow might then be considered as an extreme limiting case of the latter. This is not to say that these subgroups are not important as individual groupings, but that they all have characteristics of their parent group. That is, annular and bubbly flows can be dynamically characterized by generally low amplitude void and pressure fluctuations at the two extremes of near-liquid and near vapor behavior. On the other hand, slug-like flows are characterized by large amplitude fluctuations characteristic of periodic space-time oscillations between the two, and containing features of each. In addition, it is desirable to have groupings which can be objectively classified such as presented herein. It is simply not possible, in general, at this time to objectively determine lines of demarcation between near-neighbor subsets. The one exception to the author's knowledge is the slip ratio which has been found by Jones (1973) to reach a relatively strong maximum in the vicinity of the plain annular-mist annular transition.

Models of bubbly and annular flows have been completed by a number of investigators. The fact that slug flow appears from these experiments to be a periodical, time combination of the other two regimes, makes the idea of a combined model for slug flow quite appealing. As discussed by Jones (1973), several parameters might be correlated on this basis and some data existing in the literature exhibit these trends. The fact that the film thickness in the major bubbles in slug flow is indistinguishable from the film thicknesses obtained in plain annular flows supports the conclusion. What is not typical of general engineering systems is that a transition region can occupy the majority of the working region as in this case slug-like flows occupy the void fraction region between ~0.2 and ~0.8. While such a conclusion may not be particularly surprising, it nevertheless has not to the authors' knowledge been previously recognized or stated. The analytical implications are significant in the possible reduction in the effort required to obtain phenomena-based predictions to engineering parameters spanning these regions.

## REFERENCES


AKAGAWA, K. 1964 Fluctuations of void ratio in two-phase flow. *Bull. J.S.M.E.*, **7**, 122–128.

AKAGAWA, K., HOMAGUCHI, H., SAKAGUCHI, T. & IKARI, T. 1971 Studies on the fluctuation of pressure drop in two-phase slug flow. *Bull. J.S.M.E.*, **14**, 447–469.

DELHAYE, J. M. 1969 General Equations of Two-Phase Systems and Their Application to Air–Water Bubble Flows and to Steam–Water Flashing Flow, ASME Paper No. 69-HT-63, National Heat Transfer Conference, Minn.

GOVIER, G. W. & AZIZ, K. 1972 *The Flow of Complex Mixtures in Pipes.* Von Nostrand–Reinhold.

HARMS, A. A. & FORREST, C. F. 1971 Dynamic effects in radiation diagnosis of fluctuating voids. *Nucl. Sci. Engng* **46**, 408–413.

HEWITT, G. F. & LOVEGROVE, P. C. 1969 Frequency and Velocity Measurements of Disturbance Waves in Annular Two-Phase Flow, AERE-R 4304.

HEWITT, G. F., HUTCHINSON, P. & DUKLER, A. E. 1970 Deposition of Liquid or Solid Dispersions from Turbulent Gas Streams: A Stochastic Model, AERE-R-6637.

ISHAGAI, S., YAMANE, M. & ROKO, K. 1965 Measurement of the component flows in a vertical, two-phase flow by making use of the pressure fluctuations. *Bull. J.S.M.E.* **8**, 375–390.

JONES, O. C. 1970 Determination of Transient Characteristics of an X-ray Void Measurement System for Use in Studies of Two-Phase Flow. General Electric Co. Report, KAPL-3859.

JONES, O. C. 1973 Statistical considerations in heterogeneous two-phase flowing systems, Ph.D. Thesis. Rensselaer Polytechnic Institute.

KOCAMUSTAFAOGULLARI, G. 1971 Thermo-fluid dynamics of separated two-phase flow, Ph.D. Thesis. Georgia Institute of Technology.

LACKME, C. 1964a Statistical Analysis of the Local Structure of a Two-Phase Flow, ANL-trans-171 and ANL-trans-172.

LACKME, C. 1964b Analyse Statistique de la Structure Local d'un Ecoulement Diphase, I. Description des Arrivees de Bulles, CNS note TT 162.

LACKME, C. 1964c Analyse Statistique de la Structure Local d'un Ecoulement Diphase, II. Changement de Configuration et Distribution des Arrivees de Bulles, CEN Grenoble note TT 176.

MOISSIS, R. 1962 The Transition from Slug to Homogeneous Two-Phase Flow, ASME paper No. 62-WA-115, presented at the Winter Annual ASME meeting.

NEAL, L. G. & BANKOFF, S. G. 1963 A high resolution resistivity probe for determination of local void properties in gas-liquid flow. *A.I.Ch.E. Jl.* **9**, 490–494.

TELLES, A. S. & DUKLER, A. E. 1970 Statistical characteristics of thin, vertical wavy liquid films. *Ind. Engng Chem. Fund.* **9**, 412–421.

WALLIS, G. B. & COLLIER, J. G. 1968 Two-Phase Flow and Heat Transfer. Notes from a summer course given at Dartmouth College.

**Résumé**—Un système de mesure du taux de vide par rayons x, linéarisé et à faible temps de réponse, a été utilisé pour obtenir des propriétés statistiques d'un écoulement eau–air fluctuant naturellement dans une conduite rectangulaire. On démontre que la fonction densité de probabilité (PDF) des fluctuations du taux de vide peut être utilisée pour caractériser objectivement et quantitativement la configuration d'écoulement, et ce, pour les trois principales configurations, à bulles, à bouchons, et annulaire. Ce concept est appliqué aux résultats expérimentaux pour des vitesses du mélange couvrant la gamme 0–36 m/s, afin de montrer que l'écoulement à bouchons est une simple combinaison périodique de transition entre écoulements à bulles et annulaire. Les épaisseurs de film calculées à partir des résultats de la PDF sont en bon accord pour les deux configurations d'écoulement à bouchons et annulaire. Le calcul des longeurs de bouchons, du rapport des temps de présence, ainsi que celui des longueurs de bulles dans l'écoulement à bouchons s'obtient aussi facilement à partir des mesures statistiques. Les mesures de la densité spectrale ont montré que les écoulements à bulles sont stochastiques tandis que les écoulements à bouchons et annulaire possèdent un caractère périodique, les fréquences pouvant être correlées en fonction du flux volumique du liquide.

**Auszvg**—Es wurde ein schnell ansprechendes linearisiertes X-Strahlensystem zur Hohlraummessung fuer statistische Messungen in normal fluktuierender Luft-Wasserstroemung in einem rechteckigen Kanal eingesetzt. Es wird gezeigt, dass die Wahrscheinlichkeitsdichtenfunktion (DPF) der Schwankungen des Hohlraumanteils als objektives und quantitatives Kriterion fuer die drei Hauptformen der Blasen-, Pfropfen-, und Ringstroemung brauchbar ist. Diese Auffassung wird auf Daten im Bereich von Mischungsgeschwindigkeiten in der Groesse von 0·0 bis 37 m/s angewandt, um zu zeigen, dass Pfropfenstroemung einfach eine mit der Zeit periodische Uebergangskombination von Blasen- und Ringstroemung darstellt. Mit den PDF-Daten berechnete Schichtdickenwerte stimmen sowohl fuer Pfropfen- wie Ringstroemungen ueberein. Ebenso sind Berechnungen von Pfropfenlaengen und Verweilzeitverhaeltnissen, wie auch von Blasenlaengen in Pfropfenstroemung, leicht anhand der statistischen Messungen ausfuehrbar. Messungen des Dichtespektrums zeigten, dass Blasenstroemung stochastischer Natur ist, waehrend Pfropfen- und Ringstroemungen Periodizitaeten aufweisen, die mit dem Volumenfluss der Fluessigkeit korrelierbar sind.

**Резюме**—Для статистических измерений нормалью-флуктуирующего потока воды с воздухом в прямоугольном канале была применена быстродействующая рентгенодефектоскопическая аппаратура. Показано, что функция вероятностного распределения колебаний меры несплошности может быть использована как объктивное количественное средство различения трех основных моделей такого потока: пузырьковой, импульсной и кольцевой. Эта идея была приложена к данным обуказанной смеси, скорости которой изменялись в пределах от 0, 0 до 120 футов в секунду (до 36 м/сек) с тем, чтобы показать, что пульсирующее течение есть не что иное, как переходная, периодическая во времени комбинация пузырькового и кольцевого течений. Толщины пленок, расситанные по данным упомянутого вероятностного распределения, согласуются сак с пульсирующим, так и с кольцевым течениями. Рассчет отношений длины импульса и продолжительности вместе с выполним по разультатам статистических измерений. Измерения спектральной плотности показывают, что пузырьковое течение является случайным, в то время как пульсирующее и кольцевое течения показывают взаимосвязанную периодичность объмного тока жидкости.